

Joint Analysis of Social and Item Response Networks with Latent Space Models ^{*}

Selena Shuo Wang, Department of Psychology
Subhadeep Paul, Department of Statistics
Jessica Logan, Department of Educational Studies
Paul De Boeck, Department of Psychology
The Ohio State University

April 23, 2022

Abstract

The adjustment of students to a school environment is fundamentally linked to the friendship networks they form with their peers. Consequently, the complete picture of a student's adjustment can only be obtained by taking into account both their friendship network and their reported perceptions of the school environment. However, there is a lack of flexible statistical models and methods that can jointly analyze a social network with an item-response data matrix. In this paper, we propose a latent space model for heterogeneous (multimodal) networks (LSMH) and its extension LSMH-Item, which combine the framework of latent space modeling in network analysis with item response theory in psychometrics. Using LSMH, we summarize the information from the social network and the item responses in a person-item joint latent space. We use a Variational Bayesian Expectation-Maximization estimation algorithm to estimate the item and person locations in the joint latent space. This methodology allows effective integration, informative visualization and prediction of social networks and item responses. We apply the proposed methodology to data collected from 16 third-grade classrooms comprised of 451 third-grade students' self-reported friendships and school liking, which were collected as part of the Early Learning Ohio project. Through the person-item joint latent space, we are able identify students with potential adjustment difficulties and found consistent connection between students' friendship networks and

**The research reported here was supported by Institute for Education Sciences, through Grant R305N160024 awarded to The Ohio State University (PI Justice) and by a grant from National Science Foundation under Grant No. DMS 1830547 (PI Paul). The opinions expressed are those of the authors and do not represent views of the Institute for Education Sciences or National Center for Education Research. We would like to thank the research team, staff, and families without whom this research would not have been possible. The authors would like to thank Prof. Vishesh Karwa of Temple University and Prof. Srijan Sengupta of Virginia Tech University for discussions that helped in conceptualizing the statistical models.*

their well-being. We believe that using LSMH, researchers will be able to easily identify students in need of intervention and revolutionize the the understanding of social behaviors.

Keywords: Multimodal Heterogeneous Networks, Multidimensional Item Response Theory, Item Responses, Social Networks, Latent Space Models, School Adjustment

1 Introduction

Understanding interactions among sets of entities, often represented as complex networks, is a central research task in many data-intensive scientific fields, including: Statistics, Machine learning, Physics, Biology, Psychology, and Economics [74, 6, 3, 35, 29, 71, 13, 18, 62]. However, an overwhelming majority of methodological and applied studies have only considered interactions of one type among a set of entities of the same type. More recent studies have pointed to the heterogeneous and multimodal nature of such interactions, whereby a complex networked system is composed of multiple types of interactions among entities that themselves are of multiple types [42, 16, 56, 58, 59, 67, 72, 50, 26, 32, 57].

Social relationships are known to affect individual outcomes including dementia [27], decision making [39], adolescent smoking [55], and online behavior choices [45]. At the same time, individual attributes, such as race, age, and gender can affect whether and how people form friendships or romantic partnerships [21, 53]. The effect of social relationships on individual outcomes and its reciprocal are observable through disparities in the item responses across different individuals when their friendship structures differ and through disparities in the friendship structures when individuals' attributes differ, respectively. Therefore, a flexible joint modeling of the social relationships and the individual outcomes is needed in order to effectively investigate their interrelationships.

In recent years, the integration of network analysis with psychometrics has gained new ground, yet a flexible modeling of both social networks and item responses is still lacking. *Network Psychometrics*, as the name suggests, is a framework that connects network analysis with psychometrics by treating variables as nodes and pairwise correlations as edges [17, 66, 24]. Under this framework, an ising model is shown to be statistically equivalent to an

item response theory (IRT) model, and therefore a similar fit to the data is obtained when applying the two different models [51]. Though it is an important framework that bridges a gap between network analysis and psychometrics, *network psychometrics* can not be used to jointly model social networks and individual outcomes. A recent development in this effort is [49], which allows latent personality traits as covariates in a structural equation model. Unlike [49]’s approach converting item responses to latent factors, we propose a model that preserves item-level information using IRT. Our method is also different from [37]’s recent integration of network analysis with IRT to estimate IRT’s item and person parameters. While only item responses are model through their approach, both social networks and item responses are modeled through our approach, and thus the relationship between social relationships and individual outcomes can be examined.

A joint modeling of social networks and item responses is needed to study students’ school adjustment in relation to their friendship. It is well known that friendship structures affect students’ school adjustment [47, 48, 46, 25, 5, 41]. For example, close friendships with same-aged peers promote positive school attitude and academic performance [11, 75]. Students with at least one friend show higher academic accomplishments compared to students without friends [75]. Friendships that provide emotional support promote classroom involvement, while friendships with conflicts exacerbate school adjustment problems in childhood [47] and early adolescence [11]. School adjustment also affects friendship formation as students choose academically similar friends [40, 60, 70]. In particular, it is shown that students who adjust well in schools befriend other academically-oriented students, whereas less academically-oriented students tend to befriend those who are similarly disengaged [63]. Though there is extensive literature that investigates the relationships between school adjustment and friendships, statistical models that effectively identify students with potential adjustment difficulties while simultaneously using both social networks and students’ survey responses are lacking. In addition, previous studies often use univariate summary measures, like density of the friendship network or the number of friends each student has, to simplify the analysis of friendship networks, thus failing to explore the rich information and dependence structure associated with such complex networks.

To directly connect the analysis of social networks with the analysis of item responses,

we introduce the latent space random graph model for heterogeneous networks (LSMH) and its extension for item diagnosis (LSMH-I), which jointly analyze students' friendship networks and their school adjustment survey results. LSMH and LSMH-I retain information from friendship networks in their totality, and therefore provide more nuance when studying friendship structures and their relations to school adjustment. Using LSMH and LSMH-I, we create a joint latent space, in which estimated latent item and person positions abide by same geometric rules, for items and persons to coexist and interact. In other words, the latent item positions are determined by the information from the friendship networks and the item responses. Similarly, the latent person positions are determined by the information from both social networks and item responses. The LSMH can be used to effectively identify students with potential adjustment difficulties and to understand how students' friendships might influence their school adjustment, or vice versa. Using LSMH-I, we calculate the item difficulty and discrimination parameters taking into account both social networks and item responses.

The remainder of this paper is organized as follows. In section 2, we introduce the motivating application and the school adjustment data. In section 3 we introduce our models. Section 4 describes the estimation approach. Section 5 presents a simulation study and Section 6 applies the proposed methodology to the school adjustment data. Finally, in Section 7 we summarize our findings and discuss its extensions and future directions.

2 Classroom friendship and school adjustment data from the Early Learning Ohio project

Understanding the relationship between friendships and school adjustment from the data collected from the Early Learning Ohio project is our motivation for proposing the LSMH methodology. We start by briefly describing the data collected.

Classrooms

The sample in this study is drawn from a larger study called Early Learning Ohio, which was developed in part to investigate how children grow and change in their academic skills from pre-kindergarten through third grade. All research was conducted with the approval of the Institutional Review Board. Teachers were recruited through informational meetings with project personnel that took place at their schools. Every child in an enrolled teacher's classroom was eligible for participation, and was asked to participate via an informational packet sent home to caregivers. On average, 80% of children per classroom were enrolled in the study. Children who were not consented did not participate in the child interviews. However when collecting information about the social network, children were able to nominate any child in the class as a friend, regardless of whether the child was an active study participant.

Current Sample

The sample in this study focuses on 16 selected third-grade classrooms from one school district, located near central Ohio. Classrooms spanned urban, suburban, and rural schools. The number of students in each classroom ranges between 20 and 33.

Procedures for data collection

To incentivize participation in the study, caregivers received 10 dollars after completing a family questionnaire, and enrolled children received age appropriate books at assessment periods in fall and spring. Children were assessed in a quiet area of their school by a trained field assessor in the fall and spring. Data used in the present study were collected via child interviews, which were conducted by trained and experienced assessors to ensure accurate and reliable administration.

Measures

The social network measure was collected during an individual interview between a student and a project-based assessor. The assessor provided the student with a list of the

names of all of the children in his or her classroom, and asked the child to indicate who they liked to play with the most. Children’s responses were recorded, and an individual matrix of connections was used as the basis for the social networks examined in this study. The child interview questionnaire consisted of 23 items in 4 sub-scales: three items measuring the negative student experiences, eleven items measuring students’ perceived peer social support, six items measuring how much students like school, three items measuring how lonely the students are. These items are based on *Student Experience scale*, *Perceived Peer Social Support Scale: The peer support at school scale*, and *School Liking Questionnaire* from [14]. The students were asked to indicate whether their experience on each item was Never (0), Sometimes (1) or A Lot (2).

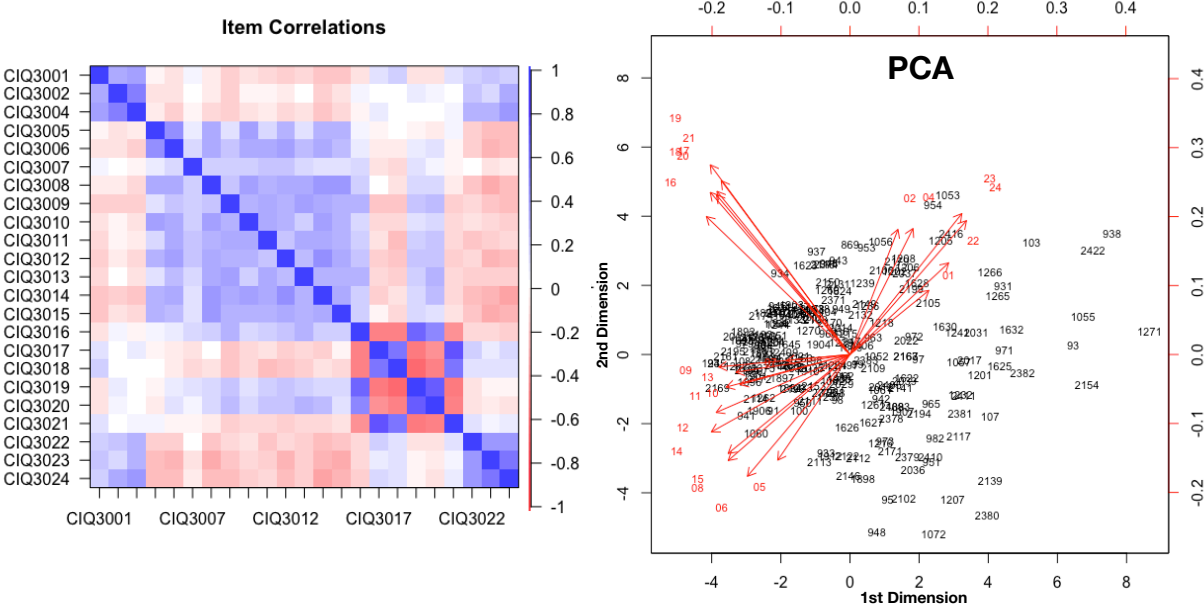


Figure 1: (A) Correlations of items across all students (B) Principal Component Analysis of item sample correlation matrix

In Figure 1 (A), we present the collective responses of the 451 students by showing the correlations of the items. The items were designed to measure four psychological construct, namely: negative student experience, perceived peer social support, school-liking, and loneliness. Three of the four sub-scales consist of items associated with only one type of emotional affect, i.e., either a positive affect or a negative affect. There are only negative items in the negative student experience and loneliness sub-scales and only positive items in the perceived

peer social support sub-scale. There are both negative and positive items in fourth sub-scale, corresponding to school-liking. The consistency of the emotional affect in one sub-scale helps us reduce the complexity of and interpret the dimensions in the students’ responses to the child interview questionnaire. Therefore, we re-coded the negative items (items 17, 18 and 21) in the school-liking sub-scale to maintain its overall positive affect.

The dimensions in the students’ responses were examined using a principle component analysis (PCA). The results show that 25.39%, 13.60% of the variability in the questionnaire responses are explained by the first two components, respectively. In Figure 1(B), we show the bi-plot of these two components. As can be seen, items in the same sub-scale are positioned in similar directions. In particular, items 1,2 and 4 (the negative student experience items) are positioned in the similar directions as items 22, 23 and 24 (the loneliness items). Together, they can be seen as items of negative emotional affect (the NEA items). If we rotate the co-ordinate axes by 45 degrees clockwise, then the NEA items are differentiated from the perceived social support (PSS) items (items 5–15) by the first dimension of the new co-ordinate axes. We refer to this dimension as the NEA dimension since a student’s positive position on this dimension indicates a high score on the NEA items and a low score on the PSS items. The school liking (SL) items (items 16–21) are positioned in the same direction as the second dimension of the new co-ordinate axes. We refer to this dimension as the SL dimension since a student’s positive position on this dimension indicates a high score on SL items. We believe that the NEA and SL dimensions give us meaningful interpretations of the students’ responses, and we aim to discover similar dimensions in the joint latent space model using LSMH.

3 Latent Space Model for Heterogeneous Networks

Consider a more general yet similar scenario as the Early Learning Ohio Project, where data are collected from a group of individuals about their friendships, and also their attitudes or behavioral outcomes using a set of survey or test questions. Optionally, additional information about the items, e.g. their relations to each other, can also be found. Under such a scenario, the data can be represented as a heterogenous multimodal network. In this

section, we propose a latent space model, LSMH to model such heterogeneous multimodal networks. Though modeling social networks and item-response networks is our primary focus in this paper, LSMH can also be used to model general heterogenous multimodal networks.

Let \mathbf{Y}_I denote the $N \times N$ adjacency matrix of the social network among N individuals. The (i, j) th element of the matrix \mathbf{Y}_I , denoted as y_{ij}^I is 1 if person i and person j are related, for $i, j = \{1, 2, \dots, N\}$ and $i \neq j$. Similarly, let \mathbf{Y}_A be the $M \times M$ adjacency matrix of the item relationship network among M items, whose (a, b) th element, denoted as y_{ab}^A is 1 if items a and b are related, for $a, b = \{1, 2, \dots, M\}$ and $a \neq b$. Finally, let \mathbf{Y}_{IA} denote the $N \times M$ item response matrix, whose (i, a) th element y_{ia}^{IA} is 1 if person i responded positively or correctly (depending upon context) to item a in the survey, for $i = \{1, 2, \dots, N\}$ and $a = \{1, 2, \dots, M\}$.

A multimodal network can be equivalently represented as a supra-adjacency matrix [43]. We define an item-person supra-adjacency matrix as a block matrix that has the friendship network adjacency matrix \mathbf{Y}_I and the item relationship adjacency matrix \mathbf{Y}_A in the diagonal blocks and the item response matrix \mathbf{Y}_{IA} and its transpose \mathbf{Y}_{IA}^T in the off-diagonal blocks (see Figure 2 (A)).

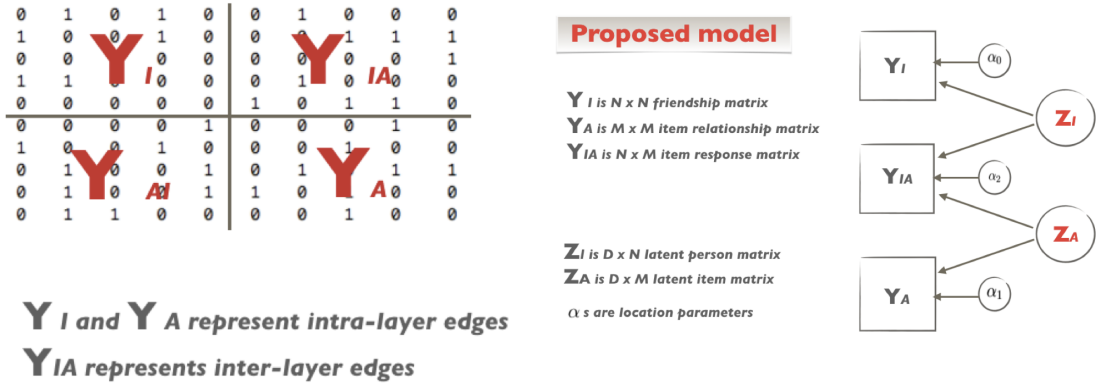


Figure 2: (A) item-person supra-adjacency matrix

(B) The LSMH

Using the proposed model LSMH, we define a item-person joint latent space as a hypothetical multidimensional space, in which the locations of the persons and the items follow predefined geometric rules reflecting each node's connection with another. Our formulation of the joint latent space is motivated by merging the philosophy of Latent Space Model

(LSM) framework with that of the Multidimensional Item-Response Theory (MIRT). The LSM framework allows us to specify and interpret the interactions among persons, whereas the MIRT framework allows us to model the items into the same latent space as the persons, i.e. the joint latent space. Next we briefly review the LSM and MIRT frameworks and then introduce our model.

The Latent Space Model

The LSM, introduced by [34] assumes that each node i has a latent position $\mathbf{z}_i = (z_{i,1}, z_{i,2}, \dots, z_{i,D})^T$ in a D -dimensional Euclidean latent space [31, 30, 68, 65, 64, 44, 28] and that the probability of node i and node j forming a connection depends on the distance between them in the latent space. The greater the distance is between two latent positions, the less likely they form a connection. In [34], the Euclidean distance $|\mathbf{z}_i - \mathbf{z}_j|$ was proposed as the distance measure of undirected networks, and the projection distance $\frac{\mathbf{z}_i \mathbf{z}_j}{|\mathbf{z}_j|}$ was proposed as the distance measure of directed networks. Extensions of [34]’s original latent space models have been proposed in literature. In [31], a mixture of Gaussian distributions was proposed to model the distribution of the latent variables \mathbf{z}_i instead of only one Gaussian distribution in order to account for possible community structures. A node specific random effect was included by [44] to model the nodes’ differing “propensity” to form ties. This model was extended to multiple networks by [30] and to bipartite networks by [28].

The Multidimensional Item Response Theory

The multidimensional item response theory (MIRT) model, as a multidimensional two-parameter logistic model [61], is a member of the intensively studied model in psychometrics—namely, the Item Response Theory (IRT) model (e.g. [23, 54, 73]).

IRT, unidimensional or multidimensional, are models that mathematically represent locations of persons in a hypothetical multidimensional space using the persons’ responses to a set of items. To achieve this, it is assumed by [61] that persons can be ranked on each of the D dimensions that individuals differ. Under this assumption, person i is attributed a latent vector of D personal characteristics, $\mathbf{z}_i = (z_{i,1}, z_{i,2}, \dots, z_{i,D})$. Using this latent vector, we describe the attributes of the person evaluated by the items, which is conceptually dif-

ferent from the latent vector in LSM. Similarly, item a , $a = 1, 2, \dots, M$ is represented by a latent vector of D item characteristics, $\mathbf{z}_a = (z_{a1}, z_{a2}, \dots, z_{aD})$. In the MIRT framework, an item can be assessed of its threshold (also called difficulty in an ability test) and sensitivity with respect to the respondents through the estimated item difficulty and discrimination parameters.

3.1 The LSMH model

In this section, we define the latent space model for heterogeneous networks (LSMH). We assume that the persons and items can be positioned in an item-person joint latent space, which is a subset of the D dimensional Euclidean space \mathbb{R}^D . Let \mathbf{Z}_I be a $N \times D$ matrix of latent person positions, each row of which is a D dimensional vector $\mathbf{u}_i = (u_{i1}, u_{i2}, \dots, u_{iD})$ indicating the latent position of person i in the Euclidean space. Similarly, let \mathbf{Z}_A be a $M \times D$ matrix of latent item positions, each row of which is a D dimensional vector $\mathbf{v}_a = (v_{a1}, v_{a2}, \dots, v_{aD})$ indicating the latent position of item a in the Euclidean space. As shown in Figure 2 (B), LSMH is used to estimate the latent person and item positions \mathbf{Z}_I and \mathbf{Z}_A using three data matrices: the friendship network \mathbf{Y}_I , the item relationship matrix \mathbf{Y}_A and the item response matrix \mathbf{Y}_{IA} . The data matrices \mathbf{Y}_I and \mathbf{Y}_A are modeled borrowing the philosophy of the LSM framework, and the data matrix \mathbf{Y}_{IA} is modeled borrowing the philosophy of the MIRT framework. In LSMH, we extend the conditional independence assumption of LSM and MIRT by assuming that the probability of forming any connection in an item-person supra-adjacency matrix is independent of all other connections given the latent positions of the two nodes involved.

In LSMH, the joint distribution of the elements of the item-person supra-adjacency matrix can be written as

$$\begin{aligned}
 p(\mathbf{Y}_I, \mathbf{Y}_A, \mathbf{Y}_{IA} | \mathbf{Z}_I, \mathbf{Z}_A, \alpha_0, \alpha_1, \alpha_2) &= \prod_{i=1}^N \prod_{j=1, j \neq i}^N p_1(y_{i,j}^I | \theta_{i,j}^I) \prod_{a=1}^M \prod_{b=1, b \neq a}^N p_2(y_{a,b}^A | \theta_{a,b}^A) \prod_{i=1}^N \prod_{a=1}^M p_3(y_{i,a}^{IA} | \theta_{i,a}^{IA}), \\
 E(y_{i,j}^I | \theta_{i,j}^I) &= g_1(\theta_{i,j}^I), & E(y_{a,b}^A | \theta_{a,b}^A) &= g_2(\theta_{a,b}^A), & E(y_{i,a}^{IA} | \theta_{i,a}^{IA}) &= g_3(\theta_{i,a}^{IA}), \\
 \theta_{i,j}^I &= \alpha_0 - |\mathbf{u}_i - \mathbf{u}_j|^2, & \theta_{a,b}^A &= \alpha_1 - |\mathbf{v}_a - \mathbf{v}_b|^2, & \theta_{i,a}^{IA} &= \alpha_2 + \mathbf{u}_i^T \mathbf{v}_a,
 \end{aligned} \tag{1}$$

where $g_i(\cdot)$ are the link functions, and $p_i(\cdot | \cdot)$ are the parametric families of distributions suit-

able for the type of data in the supra-adjacency matrix. We set the priors $\mathbf{u}_i \stackrel{iid}{\sim} N(0, \lambda_0^2 \mathbf{I}_D)$, and $\mathbf{v}_a \stackrel{iid}{\sim} N(0, \lambda_1^2 \mathbf{I}_D)$. $\alpha_0, \alpha_1, \alpha_2, \lambda_0^2, \lambda_1^2$ are unknown parameters that need to be estimated.

If the data in \mathbf{Y}_I , \mathbf{Y}_A and \mathbf{Y}_{IA} are binary, then the link functions $g_1(\theta_{i,j}^I)$, $g_2(\theta_{a,b}^A)$ and $g_3(\theta_{i,a}^{IA})$ are inverse logistic link functions, i.e., $g_1(\theta_{i,j}^I) = \frac{\exp(\alpha_0 - |\mathbf{u}_i - \mathbf{u}_j|^2)}{1 + \exp(\alpha_0 - |\mathbf{u}_i - \mathbf{u}_j|^2)}$, $g_2(\theta_{a,b}^A) = \frac{\exp(\alpha_1 - |\mathbf{v}_a - \mathbf{v}_b|^2)}{1 + \exp(\alpha_1 - |\mathbf{v}_a - \mathbf{v}_b|^2)}$, and $g_3(\theta_{i,a}^{IA}) = \frac{\exp(\alpha_2 + \mathbf{u}_i^T \mathbf{v}_a)}{1 + \exp(\alpha_2 + \mathbf{u}_i^T \mathbf{v}_a)}$, and the $p_i(\cdot|\cdot)$ are Bernoulli PDFs.

While it is common for the edges in the friendship networks to be binary, the data in the item response matrix can be more general. If the data in \mathbf{Y}_{IA} are of discrete numerical scales, they can be modeled with other parametric families. For example, we can use $g_2(\theta_{i,a}^{IA}) = \exp(\alpha_2 + \mathbf{u}_i^T \mathbf{v}_a)$ as the inverse Poisson link function to model count data in \mathbf{Y}_{IA} , and thus $p_3(y_{i,a}^{IA}|\theta_{i,a}^{IA})$ becomes the PDF of the Poisson distribution. Alternatively, we can model the presence (or absence) of an edge separately from the weight of the edge (if it is present). For example, a zero inflated normal distribution was used by [69] to model weighted edges, and the same goal was achieved by [1] using a combination of a Bernoulli distribution and a non-parametric weight distribution.

In a similar fashion, LSMH can be used to handle weighted edges. A zero inflated Poisson model for the distribution of $y_{i,a}^{IA}|\theta_{i,a}^{IA}$ can be seen as follows:

$$p_3(y_{i,a}^{IA}|\theta_{i,a}^{IA}) = (1 - (\kappa(\theta_{i,a}^{IA}))^{(y_{i,a}^{IA}=0)}) \times \left\{ (\kappa(\theta_{i,a}^{IA})) \prod \frac{\exp(-\gamma(\theta_{i,a}^{IA})) \gamma(\theta_{i,a}^{IA})^{y_{i,a}^{IA}}}{y_{i,a}^{IA}!} \right\}$$

$$\kappa(\theta_{i,a}^{IA}) = \frac{\exp(\alpha_2 + \mathbf{u}_i^T \mathbf{v}_a)}{1 + \exp(\alpha_2 + \mathbf{u}_i^T \mathbf{v}_a)}$$

$$\gamma(\theta_{i,a}^{IA}) = \exp(\alpha_2 + \mathbf{u}_i^T \mathbf{v}_a).$$

In LSMH, we use the squared Euclidean distances $|\mathbf{u}_i - \mathbf{u}_j|^2$ and $|\mathbf{v}_a - \mathbf{v}_b|^2$ instead of the Euclidean distance. It is shown by [30] that squared Euclidean distances are computationally more efficient and that the latent positions obtained using squared Euclidean distances are extremely similar to those obtained using Euclidean distances. In LSMH, we also use a global scalar intercept instead of an item vector intercept, which is the functional form of MIRT to model the Y_{IA} matrix. In the next section, we retain the item vector intercept and introduce the latent space model with item intercept, the LSMH-I.

The item relationship matrix comes from an exogenous source of information regarding

items, independent from the item response matrix and the friendship network. For example, an item relationship matrix can be obtained from previously known correlations of items. Alternatively, the latent item and person positions can be estimated without the information in Y_A in that \mathbf{u}_i s and \mathbf{v}_a s can be estimated without $f(\mathbf{Y}_A|\mathbf{Z}_A, \alpha_1)$ in Equation 1. To model students’ adjustment well-being within their classroom, we use Y_A to incorporate responses from students outside of their classroom, and thus our \mathbf{Y}_A comes from an exogeneous source of information, independent from \mathbf{Y}_I or \mathbf{Y}_{IA} .

In LSMH, the interactions among persons and the connections among items are interpreted following the LSM distance framework. The probability of person i and person j forming a friendly connection depends on the distance of \mathbf{u}_i and \mathbf{u}_j in the joint latent space. The smaller the latent distance between person i and j , the higher the chance that person i and person j are friends. Similarly, the closer the latent positions of item a and b are, the more likely that item a and b measure the same individual attitudes or attributes. The relationships among persons and the connections among items also retain the transitivity and reciprocity properties of the LSM: if person i and j form a bond, and person i and k are also friends, then person j befriending person i (reciprocity), and befriending person k (transitivity) are both more likely. The same is true for relationships among items.

The interactions among persons and items are interpreted following the latent space projection model framework [34]. In the latent space projection model framework, we reparameterize $\mathbf{u}_i^T \mathbf{v}_a$ with unit-length D -dimensional vectors \mathbf{w}_i , \mathbf{w}_a , and scalars c_i , c_a . Let $\mathbf{u}_i = c_i \mathbf{w}_i$ and $\mathbf{v}_a = c_a \mathbf{w}_a$. Then $\mathbf{u}_i^T \mathbf{v}_a = c_i c_a \mathbf{w}_i^T \mathbf{w}_a$, which is the signed magnitude of the projection of \mathbf{u}_i in the direction of \mathbf{v}_a ($c_a \mathbf{w}_i^T \mathbf{w}_a$) multiplied by c_i . The projection of \mathbf{u}_i in the direction of \mathbf{v}_a can be interpreted as the extent to which item a measures the attitudes and attributes of person i . The angle between \mathbf{w}_i and \mathbf{w}_a captures the “similarity” between person i and item a . Item a and person i are favorable to having ties when \mathbf{w}_i and \mathbf{w}_a are in the same direction, i.e. $\mathbf{w}_i^T \mathbf{w}_a > 0$; are averse to having ties when \mathbf{w}_i and \mathbf{w}_a are in the opposite directions, i.e. $\mathbf{w}_i^T \mathbf{w}_a < 0$; and are neutral to having ties when the angle is a right angle, i.e. $\mathbf{w}_i^T \mathbf{w}_a = 0$. The magnitudes of c_i and c_a capture the activity levels of node i and a [34].

According to [61], a coordinate system is necessary to specify the locations of the items

and the persons for any model development, but the coordinates themselves do not always coincide with meaningful dimensions. This arbitrariness of coordinate system is seen in our item-person joint latent space. Each dimension of the coordinate system is found through the optimization procedures, therefore can seem arbitrary at times. Using an arbitrary set of coordinates to describe constructs is quite common. Yet, the arbitrariness of the coordinates does not limit our interpretations of the relative positions and inter-relationships of the persons and items in the joint latent space.

3.2 The LSMH with Item Intercept (LSMH-I)

We propose an extension of the model in Equation 1 by replacing the scalar intercept α_2 with a vector of item specific “fixed effects”, $\boldsymbol{\beta}$ of length a . We call this model LSMH-I.

$$\theta_{i,a}^{IA} = \beta_a + \mathbf{u}_i^T \mathbf{v}_a, \quad (2)$$

where β_a is the a th element in vector $\boldsymbol{\beta}$. In LSMH-I, the β_a parameters are used to model the inherent “properties” of the items and are similar to the “degree correction” parameters in the degree corrected stochastic block models [77] or the “sociability” parameters in the latent space models [44]. In LSMH-I, we also directly incorporate the functional form of MIRT, which allows us to estimate item difficulty and discrimination parameters while taking into account students’ friendship information.

In this paper, we follow [61]’s notation and use A_a and B_a to summarize the item discrimination and difficulty information in the multidimensional space. In [61], A_a is used as the multidimensional discrimination for item a , which is also MDISC_a in other articles. B_a is used to represent the multidimensional difficulty of item a , which is also represented by MDIFF . Regardless of the notations, an item with higher discrimination power more easily distinguishes persons with differing “ability”. A more difficult item requires higher ability of the test takers to be answered correctly. In our LSMH-I, A_a and B_a are defined as

$$A_a = \sqrt{\sum_{d=1}^D v_{ad}^2}, \quad B_a = \frac{-\beta_a}{\sqrt{\sum_{d=1}^D v_{ad}^2}}, \quad i = \{1, \dots, N\}, a = \{1, \dots, M\}$$

where v_{ad} is the coordinate of item a on dimension d and β_a is the intercept for item a . A_a and B_a relate to the item response surface (IRS), which describes the probability of a positive

answer as a function of a person’s “ability” in D dimensions. A_a represents the steepest slope of the IRS in the direction where item a is most differentiable and most sensitive. B_a is the distance from the origin to the point of steepest slope in the direction most differentiated by item a . Large values of A_a and B_a indicate a high discrimination and high difficulty of an item respectively.

Both LSMH and LSMH-I can be used to jointly summarize information in the social network and item response data. In modeling the item responses, both models retain the term $\mathbf{u}_i^T \mathbf{v}_a$. The difference is that a global item intercept is used in the LSMH, while a vector item intercept is used in the LSMH-I. If we are interested in the outcomes of the persons, it is appropriate to apply LSMH. The global intercept in the LSMH accounts for any mean differences in the estimated latent person and item positions, which allows us to readily observe how persons are responding to different items in the joint latent space. There is more reason to apply LSMH-I with large datasets as they allow us to accurately estimate the β_a parameters. Using LSMH-I, we can also estimate item discrimination and difficulty parameters that take into account the friendship information. Researchers should select the appropriate model based on the research focuses.

The primary goal of our paper is to investigate students’ adjustment well-being within each classroom using LSMH. A comprehensive study of the items using LSMH-I is also possible. We propose a LSMH-I model that takes into account the item responses for all students in different classrooms and their friendship networks within each classroom. We have C classroom friendship networks, and we use N_c to denote the number of students in the c th classroom. We use \mathbf{Y}_I^c to denote the corresponding c th classroom friendship network and use \mathbf{Y}_{IA} to denote the overall item-response matrix. Then,

$$p(\mathbf{Y}_I^1, \dots, \mathbf{Y}_I^C, \mathbf{Y}_{IA} | \mathbf{Z}_I, \mathbf{Z}_A, \alpha_1, \dots, \alpha_C, \beta_a) = \prod_{c=1}^C \prod_{i=1}^{N_c} \prod_{j=1, j \neq i}^{N_c} p(y_{i,j}^{I,c} | \theta_{i,j}^{I,c}) \prod_{i=1}^N \prod_{a=1}^M p(y_{i,a}^{IA} | \theta_{i,a}^{IA}) \quad (3)$$

$$\theta_{i,a}^{IA} = \beta_a + \mathbf{u}_i^T \mathbf{v}_a, \quad \theta_{i,j}^{I,c} = \alpha_c - |\mathbf{u}_i - \mathbf{u}_j|^2, \quad c = \{1, \dots, C\},$$

, where $N = \sum_c N_c$ is the total number of students from the C classrooms. \mathbf{u}_i and \mathbf{v}_a are the latent positions of the i th student and a th item, and α_c and β_a are the intercepts for the c th classroom and the a th item. The β_a parameters model the properties of the items,

and the α_c parameters model the variations in the density of friendship networks in different classrooms.

4 The Variational Bayesian Inference

We are interested in the posterior inference of the latent variables \mathbf{u}_i and \mathbf{v}_a conditioning on the observed data. The (conditional) posterior distribution is the ratio of the joint distribution of the observed data and unobserved latent variables to the observed data likelihood.

$$P(\mathbf{Z}_I, \mathbf{Z}_A | \mathbf{Y}_I, \mathbf{Y}_A, \mathbf{Y}_{IA}) = \frac{P(\mathbf{Y}_I, \mathbf{Y}_A, \mathbf{Y}_{IA} | \mathbf{Z}_I, \mathbf{Z}_A) P(\mathbf{Z}_I, \mathbf{Z}_A)}{P(\mathbf{Y}_I, \mathbf{Y}_A, \mathbf{Y}_{IA})}.$$

We can completely characterize the distribution of latent positions and thus obtain the point and interval estimates by computing this posterior distribution. However, to compute this conditional posterior, we need to evaluate the normalizing constant in the denominator above, which involves integration over the latent variables. This posterior distribution is therefore intractable. The variational inference algorithm is commonly used to estimate latent variables whose posterior distribution is intractable [9, 4, 8, 15]. In network analysis, the variational approach has been proposed for the stochastic blockmodel [20, 19], the mixed-membership stochastic blockmodel [2], the multi-layer stochastic blockmodel [76, 58], the dynamic stochastic blockmodel [52], the latent position cluster model [65] and the multiple network latent space model [30]. Here, we propose a Variational Bayesian Expectation Maximization (VBEM) algorithm to approximate the posterior of the person and the item latent positions in LSMH and in LSMH-I. We propose a class of suitable variational posterior distributions for the conditional distribution of $(\mathbf{Z}_I, \mathbf{Z}_A | \mathbf{Y}_I, \mathbf{Y}_A, \mathbf{Y}_{IA})$ and obtain a distribution from the class that minimizes the Kulback Leibler (KL) divergence from the true but intractable posterior.

For LSMH, we assign the following variational posterior distribution: $q(\mathbf{u}_i) = N(\tilde{\mathbf{u}}_i, \tilde{\Lambda}_0)$ and $q(\mathbf{v}_a) = N(\tilde{\mathbf{v}}_a, \tilde{\Lambda}_1)$. We set the joint distribution as

$$q(\mathbf{Z}_I, \mathbf{Z}_A | \mathbf{Y}_I, \mathbf{Y}_A, \mathbf{Y}_{IA}) = \prod_{i=1}^N q(\mathbf{u}_i) \prod_{a=1}^M q(\mathbf{v}_a),$$

, where $\tilde{\mathbf{u}}_i, \tilde{\Lambda}_0, \tilde{\mathbf{v}}_a, \tilde{\Lambda}_1$ are the parameters of the distribution, known as variational parameters.

We can estimate the variational parameters by minimizing the Kullback-Leiber (KL) divergence between the variational posterior $q(\mathbf{Z}_I, \mathbf{Z}_A | \mathbf{Y}_I, \mathbf{Y}_A, \mathbf{Y}_{IA})$ and the true posterior $f(\mathbf{Z}_I, \mathbf{Z}_A | \mathbf{Y}_I, \mathbf{Y}_A, \mathbf{Y}_{IA})$. Minimizing the KL divergence is equivalent to maximizing the following Evidence Lower Bound (ELBO) function [15], (see detailed derivations in the Supplementary Materials)

$$\begin{aligned}
\text{ELBO} &= -\mathbb{E}_{q(\mathbf{Z}_I, \mathbf{Z}_A, \alpha_0, \alpha_1, \alpha_2 | \mathbf{Y}_I, \mathbf{Y}_A, \mathbf{Y}_{IA})} \left[\frac{\log q(\mathbf{Z}_I, \mathbf{Z}_A, \alpha_0, \alpha_1, \alpha_2 | \mathbf{Y}_I, \mathbf{Y}_A, \mathbf{Y}_{IA})}{\log p(\mathbf{Z}_I, \mathbf{Z}_A, \mathbf{Y}_I, \mathbf{Y}_A, \mathbf{Y}_{IA} | \alpha_0, \alpha_1, \alpha_2)} \right] \\
&= -\int q(\mathbf{Z}_I, \mathbf{Z}_A, \alpha_0, \alpha_1, \alpha_2 | \mathbf{Y}_I, \mathbf{Y}_A, \mathbf{Y}_{IA}) \log \frac{q(\mathbf{Z}_I, \mathbf{Z}_A, \alpha_0, \alpha_1, \alpha_2 | \mathbf{Y}_I, \mathbf{Y}_A, \mathbf{Y}_{IA})}{f(\mathbf{Z}_I, \mathbf{Z}_A, \alpha_0, \alpha_1, \alpha_2 | \mathbf{Y}_I, \mathbf{Y}_A, \mathbf{Y}_{IA})} d(\mathbf{Z}_I, \mathbf{Z}_A, \alpha_0, \alpha_1, \alpha_2) \\
&= -\int \prod_{i=1}^N q(\mathbf{u}_i) \prod_{a=1}^M q(\mathbf{v}_a) \log \frac{\prod_{i=1}^N q(\mathbf{u}_i) \prod_{a=1}^M q(\mathbf{v}_a)}{f(\mathbf{Y}_I, \mathbf{Y}_A, \mathbf{Y}_{IA} | \mathbf{Z}_I, \mathbf{Z}_A, \alpha_0, \alpha_1, \alpha_2) \prod_{i=1}^N f(\mathbf{u}_i) \prod_{a=1}^M f(\mathbf{v}_a)} d(\mathbf{Z}_I, \mathbf{Z}_A, \alpha_0, \alpha_1, \alpha_2) \\
&= -\sum_{i=1}^N \int q(\mathbf{u}_i) \log \frac{q(\mathbf{u}_i)}{f(\mathbf{u}_i)} d\mathbf{u}_i - \sum_{a=1}^M \int q(\mathbf{v}_a) \log \frac{q(\mathbf{v}_a)}{f(\mathbf{v}_a)} d\mathbf{v}_a \\
&+ \int q(\mathbf{Z}_I, \mathbf{Z}_A, \alpha_0, \alpha_1, \alpha_2 | \mathbf{Y}_I, \mathbf{Y}_A, \mathbf{Y}_{IA}) \log f(\mathbf{Y}_I, \mathbf{Y}_A, \mathbf{Y}_{IA} | \mathbf{Z}_I, \mathbf{Z}_A, \alpha_0, \alpha_1, \alpha_2) d(\mathbf{Z}_I, \mathbf{Z}_A, \alpha_0, \alpha_1, \alpha_2) \\
&= -\sum_{i=1}^N \text{KL}[q(\mathbf{u}_i) | f(\mathbf{u}_i)] - \sum_{a=1}^M \text{KL}[q(\mathbf{v}_a) | f(\mathbf{v}_a)] \\
&+ \mathbb{E}_{q(\mathbf{Z}_I, \mathbf{Z}_A, \alpha_0, \alpha_1, \alpha_2 | \mathbf{Y}_I, \mathbf{Y}_A, \mathbf{Y}_{IA})} [\log f(\mathbf{Y}_I, \mathbf{Y}_A, \mathbf{Y}_{IA} | \mathbf{Z}_I, \mathbf{Z}_A, \alpha_0, \alpha_1, \alpha_2)] \\
&= -\frac{1}{2} \left(DN \log(\lambda_0^2) - N \log(\det(\tilde{\Lambda}_0)) \right) - \frac{N \text{tr}(\tilde{\Lambda}_0)}{2\lambda_0^2} - \frac{\sum_{i=1}^N \tilde{\mathbf{u}}_i^T \tilde{\mathbf{u}}_i}{2\lambda_0^2} \\
&\quad - \frac{1}{2} \left(DM \log(\lambda_1^2) - M \log(\det(\tilde{\Lambda}_1)) \right) - \frac{M \text{tr}(\tilde{\Lambda}_1)}{2\lambda_1^2} - \frac{\sum_{a=1}^M \tilde{\mathbf{v}}_a^T \tilde{\mathbf{v}}_a}{2\lambda_1^2} + \frac{1}{2} (MD + ND) \\
&+ \mathbb{E}_{q(\mathbf{Z}_I, \mathbf{Z}_A | \mathbf{Y}_I, \mathbf{Y}_A, \mathbf{Y}_{IA})} [\log f(\mathbf{Y}_I, \mathbf{Y}_A, \mathbf{Y}_{IA} | \mathbf{Z}_I, \mathbf{Z}_A)]
\end{aligned}$$

After applying Jensen's inequality [36], a lower-bound on the third term is given by,

$$\begin{aligned}
&\mathbb{E}_{q(\mathbf{Z}_I, \mathbf{Z}_A | \mathbf{Y}_I, \mathbf{Y}_A, \mathbf{Y}_{IA})} [\log f(\mathbf{Y}_I, \mathbf{Y}_A, \mathbf{Y}_{IA} | \mathbf{Z}_I, \mathbf{Z}_A, \alpha_0, \alpha_1, \alpha_2)] \\
&\geq \sum_{i=1}^N \sum_{a=1}^M y_{ia}^{IA} (\tilde{\alpha}_2 + \tilde{\mathbf{u}}_i^T \tilde{\mathbf{v}}_a) + \sum_{i=1}^N \sum_{j=1, j \neq i}^N y_{ij}^I \left[\tilde{\alpha}_0 - 2 \text{tr}(\tilde{\Lambda}_0) - (\tilde{\mathbf{u}}_i - \tilde{\mathbf{u}}_j)^T (\tilde{\mathbf{u}}_i - \tilde{\mathbf{u}}_j) \right] \\
&+ \sum_{a=1}^M \sum_{b=1, b \neq a}^M y_{ab} \left[\tilde{\alpha}_1 - 2 \text{tr}(\tilde{\Lambda}_1) - (\tilde{\mathbf{v}}_a - \tilde{\mathbf{v}}_b)^T (\tilde{\mathbf{v}}_a - \tilde{\mathbf{v}}_b) \right] \\
&- \sum_{i=1}^N \sum_{a=1}^M \log \left(1 + \frac{\exp(\tilde{\alpha}_2)}{\det(\mathbf{I} - 2\tilde{\Lambda}_0^{1/2} \tilde{\Lambda}_1^{1/2})^{1/2}} \right)
\end{aligned}$$

$$\begin{aligned}
& \exp \left(\tilde{\mathbf{u}}_i^T \tilde{\mathbf{v}}_a + \frac{1}{2} (\tilde{\Lambda}_1^{1/2} \tilde{\mathbf{u}}_i + \tilde{\Lambda}_0^{1/2} \tilde{\mathbf{v}}_a)^T (\mathbf{I} - 2\tilde{\Lambda}_0^{1/2} \tilde{\Lambda}_1^{1/2})^{-1} (\tilde{\Lambda}_1^{1/2} \tilde{\mathbf{u}}_i + \tilde{\Lambda}_0^{1/2} \tilde{\mathbf{v}}_a) \right) \\
& - \sum_{i=1}^N \sum_{j=1, j \neq i}^N \log \left(1 + \frac{\exp(\tilde{\alpha}_0)}{\det(\mathbf{I} + 4\tilde{\Lambda}_0)^{1/2}} \exp \left(- (\tilde{\mathbf{u}}_i - \tilde{\mathbf{u}}_j)^T (\mathbf{I} + 4\tilde{\Lambda}_0)^{-1} (\tilde{\mathbf{u}}_i - \tilde{\mathbf{u}}_j) \right) \right) \\
& - \sum_{a=1}^M \sum_{b=1, b \neq a}^M \log \left(1 + \frac{\exp(\tilde{\alpha}_1)}{\det(\mathbf{I} + 4\tilde{\Lambda}_1)^{1/2}} \exp \left(- (\tilde{\mathbf{v}}_a - \tilde{\mathbf{v}}_b)^T (\mathbf{I} + 4\tilde{\Lambda}_1)^{-1} (\tilde{\mathbf{v}}_a - \tilde{\mathbf{v}}_b) \right) \right)
\end{aligned}$$

We use the Variational Expectation-Maximization (EM) algorithm [38, 7, 22] to maximize the ELBO function. Following the variational EM algorithm, we replace the E step of the celebrated EM algorithm, where we compute the expectation of the complete likelihood with respect to the conditional distribution $f(\mathbf{Z}_I, \mathbf{Z}_A | \mathbf{Y}_I, \mathbf{Y}_A, \mathbf{Y}_{IA})$, with a VE step, where we compute the expectation with respect to the best variational distribution (obtained by optimizing the ELBO function) at that iteration.

The detailed procedures are as follows. We start with the initial parameter, $\Theta^{(0)} = \tilde{\alpha}_0^{(0)}, \tilde{\alpha}_1^{(0)}, \tilde{\alpha}_2^{(0)}$, and $\tilde{\mathbf{u}}_i^{(0)}, \tilde{\Lambda}_0^{(0)}, \tilde{\mathbf{v}}_a^{(0)}, \tilde{\Lambda}_1^{(0)}$, and then we iterate the following VE (Variational expectation) and M (maximization) steps. During the VE step, we maximize the $\text{ELBO}(q(\mathbf{Z}), \Theta)$ with respect to the variational parameters $\tilde{\mathbf{u}}_i, \tilde{\mathbf{v}}_a, \tilde{\Lambda}_0$ and $\tilde{\Lambda}_1$ given the other model parameters and obtain $\text{ELBO}(q^*(\mathbf{Z}), \Theta)$. During the M step, we fix $\tilde{\mathbf{u}}_i, \tilde{\mathbf{v}}_a, \tilde{\Lambda}_0$ and $\tilde{\Lambda}_1$ and maximize the $\text{ELBO}(q(\mathbf{Z}), \Theta)$ with respect to $\tilde{\alpha}_0, \tilde{\alpha}_1$ and $\tilde{\alpha}_2$. To do this, we differentiate $\text{ELBO}(q(\mathbf{Z}), \Theta)$ with respect to each variational parameter. Closed form update rules are obtained by setting the partial derivatives to zero while introducing the first- and second-order Taylor series expansion approximation of the log functions in $\text{ELBO}(q(\mathbf{Z}), \Theta)$ (see detailed derivations in supplementary material). The Taylor series expansions are commonly used in the variational approaches. For example, three first-order Taylor expansions were used by [65] to simplify the Euclidean distance in the latent position cluster model, and first- and second-order Taylor expansions were used by [30] to simplify the squared Euclidean distance in LSM. Following the previous publications using Taylor expansions, we approximate the three log functions in our $\text{ELBO}(q(\mathbf{Z}), \Theta)$ function to find closed form update rules for the variational parameters.

The three log functions are

$$\begin{aligned}
\mathbf{F}_{IA} &= \sum_{i=1}^N \sum_{a=1}^M \log \left(1 + \frac{\exp(\tilde{\alpha}_2)}{\det(\mathbf{I} - 2\tilde{\Lambda}_0^{1/2}\tilde{\Lambda}_1^{1/2})^{1/2}} \right. \\
&\quad \left. \exp \left(\tilde{\mathbf{u}}_i^T \tilde{\mathbf{v}}_a + \frac{1}{2}(\tilde{\Lambda}_1^{1/2}\tilde{\mathbf{u}}_i + \tilde{\Lambda}_0^{1/2}\tilde{\mathbf{v}}_a)^T (\mathbf{I} - 2\tilde{\Lambda}_0^{1/2}\tilde{\Lambda}_1^{1/2})^{-1} (\tilde{\Lambda}_1^{1/2}\tilde{\mathbf{u}}_i + \tilde{\Lambda}_0^{1/2}\tilde{\mathbf{v}}_a) \right) \right) \\
\mathbf{F}_I &= \sum_{i=1}^N \sum_{j=1, j \neq i}^N \log \left(1 + \frac{\exp(\tilde{\alpha}_0)}{\det(\mathbf{I} + 4\tilde{\Lambda}_0)^{1/2}} \exp \left(-(\tilde{\mathbf{u}}_i - \tilde{\mathbf{u}}_j)^T (\mathbf{I} + 4\tilde{\Lambda}_0)^{-1} (\tilde{\mathbf{u}}_i - \tilde{\mathbf{u}}_j) \right) \right) \\
\mathbf{F}_A &= \sum_{a=1}^M \sum_{b=1, b \neq a}^M \log \left(1 + \frac{\exp(\tilde{\alpha}_1)}{\det(\mathbf{I} + 4\tilde{\Lambda}_1)^{1/2}} \exp \left(-(\tilde{\mathbf{v}}_a - \tilde{\mathbf{v}}_b)^T (\mathbf{I} + 4\tilde{\Lambda}_1)^{-1} (\tilde{\mathbf{v}}_a - \tilde{\mathbf{v}}_b) \right) \right)
\end{aligned}$$

The closed form update rules of the $(t+1)$ th iteration are as follows

VE-step: Estimate $\tilde{\mathbf{u}}_i^{(t+1)}$, $\tilde{\mathbf{v}}_a^{(t+1)}$, $\tilde{\Lambda}_0^{(t+1)}$ and $\tilde{\Lambda}_1^{(t+1)}$ by minimizing $\text{ELBO}(q(\mathbf{Z}), \Theta)$

$$\begin{aligned}
\tilde{\mathbf{u}}_i^{(t+1)} &= \left[\left(\frac{1}{2\lambda_0} + \sum_{j=1, j \neq i}^N (y_{ji}^I + y_{ij}^I) \right) \mathbf{I} + \mathbf{H}_I(\tilde{\mathbf{u}}_i^{(t)}) + \frac{1}{2} \mathbf{H}_{IA}(\tilde{\mathbf{u}}_i^{(t)}) \right]^{-1} \\
&\quad \left[\sum_{j=1, j \neq i}^N (y_{ji}^I + y_{ij}^I) \tilde{\mathbf{u}}_j + \frac{1}{2} \sum_{a=1}^M y_{ia}^{IA} \tilde{\mathbf{v}}_a^{(t)} - \mathbf{G}_I(\tilde{\mathbf{u}}_i^{(t)}) \right. \\
&\quad \left. + \left(\mathbf{H}_I(\tilde{\mathbf{u}}_i^{(t)}) + \frac{1}{2} \mathbf{H}_{IA}(\tilde{\mathbf{u}}_i^{(t)}) \right) \tilde{\mathbf{u}}_i^{(t)} - \frac{1}{2} \mathbf{G}_{IA}(\tilde{\mathbf{u}}_i^{(t)}) \right] \\
\tilde{\mathbf{v}}_a^{(t+1)} &= \left[\left(\frac{1}{2\lambda_1} + \sum_{b=1, b \neq a}^M (y_{ba}^A + y_{ab}^A) \right) \mathbf{I} + \mathbf{H}_A(\tilde{\mathbf{v}}_a^{(t)}) + \frac{1}{2} \mathbf{H}_{IA}(\tilde{\mathbf{v}}_a^{(t)}) \right]^{-1} \\
&\quad \left[\sum_{b=1, b \neq a}^M (y_{ba}^A + y_{ab}^A) \tilde{\mathbf{v}}_b + \frac{1}{2} \sum_{i=1}^N y_{ia}^{IA} \tilde{\mathbf{u}}_i^{(t)} - \mathbf{G}_A(\tilde{\mathbf{v}}_a^{(t)}) \right. \\
&\quad \left. + \left(\mathbf{H}_A(\tilde{\mathbf{v}}_a^{(t)}) + \frac{1}{2} \mathbf{H}_{IA}(\tilde{\mathbf{v}}_a^{(t)}) \right) \tilde{\mathbf{v}}_a^{(t)} - \frac{1}{2} \mathbf{G}_{IA}(\tilde{\mathbf{v}}_a^{(t)}) \right] \\
\tilde{\Lambda}_0^{(t+1)} &= \left[\left(\frac{1}{\lambda_0} + \frac{\sum_{i=1}^N \sum_{j=1}^N y_{ij}^I}{N} \right) \mathbf{I} + \frac{2}{N} \mathbf{G}_I(\tilde{\Lambda}_0^{(t)}) + \frac{1}{2} \mathbf{G}_{IA}(\tilde{\Lambda}_0^{(t)}) \right]^{-1} \\
\tilde{\Lambda}_1^{(t+1)} &= \left[\left(\frac{1}{\lambda_1} + \frac{\sum_{a=1}^M \sum_{b=1}^M y_{ij}^I}{N} \right) \mathbf{I} + \frac{2}{M} \mathbf{G}_A(\tilde{\Lambda}_1^{(t)}) + \frac{1}{2} \mathbf{G}_{IA}(\tilde{\Lambda}_1^{(t)}) \right]^{-1}
\end{aligned}$$

where $\mathbf{G}_I(\tilde{\mathbf{u}}_i^{(t)})$, $\mathbf{G}_A(\tilde{\mathbf{v}}_a^{(t)})$, $\mathbf{G}_{IA}(\tilde{\mathbf{u}}_i^{(t)})$ and $\mathbf{G}_{IA}(\tilde{\mathbf{v}}_a^{(t)})$ are the partial derivatives (gradients) of \mathbf{F}_I , \mathbf{F}_A , \mathbf{F}_{IA} and \mathbf{F}_{IA} with respect to $\tilde{\mathbf{u}}_i$, $\tilde{\mathbf{v}}_a$, $\tilde{\mathbf{u}}_i$ and $\tilde{\mathbf{v}}_a$, evaluated at $\tilde{\mathbf{u}}_i^{(t)}$, $\tilde{\mathbf{v}}_a^{(t)}$, $\tilde{\mathbf{u}}_i^{(t)}$ and $\tilde{\mathbf{v}}_a^{(t)}$ respectively. In $\mathbf{G}_I(\tilde{\mathbf{u}}_i^{(t)})$, the subscript I indicates that the gradient is of function \mathbf{F}_I , and the subscript i in $\tilde{\mathbf{u}}_i^{(t)}$ indicates that the gradient is with respect to $\tilde{\mathbf{u}}_i$, evaluated at $\tilde{\mathbf{u}}_i^{(t)}$. Similarly, $\mathbf{H}_I(\tilde{\mathbf{u}}_i^{(t)})$, $\mathbf{H}_A(\tilde{\mathbf{v}}_a^{(t)})$, $\mathbf{H}_{IA}(\tilde{\mathbf{u}}_i^{(t)})$ and $\mathbf{H}_{IA}(\tilde{\mathbf{v}}_a^{(t)})$ are the second-order partial derivatives of \mathbf{F}_I , \mathbf{F}_A , \mathbf{F}_{IA} and \mathbf{F}_{IA} with respect to $\tilde{\mathbf{u}}_i$, $\tilde{\mathbf{v}}_a$, $\tilde{\mathbf{u}}_i$ and $\tilde{\mathbf{v}}_a$, evaluated at $\tilde{\mathbf{u}}_i^{(t)}$, $\tilde{\mathbf{v}}_a^{(t)}$, $\tilde{\mathbf{u}}_i^{(t)}$ and $\tilde{\mathbf{v}}_a^{(t)}$ respectively.

M-step: Estimate $\tilde{\alpha}_0^{(t+1)}$, $\tilde{\alpha}_1^{(t+1)}$ and $\tilde{\alpha}_2^{(t+1)}$ by maximizing $\text{ELBO}(q(\mathbf{Z}), \Theta)$

$$\begin{aligned}\tilde{\alpha}_0^{(t+1)} &= \frac{\sum_{i=1}^N \sum_{j=1}^N y_{ij}^I - g_I(\tilde{\alpha}_0^{(t)}) + \tilde{\alpha}_0^{(t)} h_I(\tilde{\alpha}_0^{(t)})}{h_I(\tilde{\alpha}_0^{(t)})} \\ \tilde{\alpha}_1^{(t+1)} &= \frac{\sum_{a=1}^M \sum_{b=1}^M y_{ab}^A - g_A(\tilde{\alpha}_1^{(t)}) + \tilde{\alpha}_1^{(t)} h_A(\tilde{\alpha}_1^{(t)})}{h_A(\tilde{\alpha}_1^{(t)})} \\ \tilde{\alpha}_2^{(t+1)} &= \frac{\sum_{i=1}^N \sum_{a=1}^M y_{ia}^{IA} - g_{IA}(\tilde{\alpha}_2^{(t)}) + \tilde{\alpha}_2^{(t)} h_{IA}(\tilde{\alpha}_2^{(t)})}{h_{IA}(\tilde{\alpha}_2^{(t)})}\end{aligned}$$

, where $g_I(\tilde{\alpha}_0^{(t)})$, $g_A(\tilde{\alpha}_1^{(t)})$ and $g_{IA}(\tilde{\alpha}_2^{(t)})$ are the partial derivatives (gradients) of \mathbf{F}_I , \mathbf{F}_A and \mathbf{F}_{IA} with respect to $\tilde{\alpha}_0$, $\tilde{\alpha}_1$ and $\tilde{\alpha}_2$, evaluated at $\tilde{\alpha}_0^{(t)}$, $\tilde{\alpha}_1^{(t)}$ and $\tilde{\alpha}_2^{(t)}$; and $h_I(\tilde{\alpha}_0^{(t)})$, $h_A(\tilde{\alpha}_1^{(t)})$ and $h_{IA}(\tilde{\alpha}_2^{(t)})$ are the second-order partial derivatives of \mathbf{F}_I , \mathbf{F}_A and \mathbf{F}_{IA} with respect to $\tilde{\alpha}_0$, $\tilde{\alpha}_1$ and $\tilde{\alpha}_2$, evaluated at $\tilde{\alpha}_0^{(t)}$, $\tilde{\alpha}_1^{(t)}$ and $\tilde{\alpha}_2^{(t)}$.

The VBEM approach for LSMH-I is similar to the VBEM approach for LSMH with the exception of $\tilde{\alpha}_a$, $a = 1, 2, \dots, M$ replacing $\tilde{\alpha}_2$. Therefore, the closed form update rule for $\tilde{\alpha}_a$ is

$$\tilde{\alpha}_a^{(t+1)} = \frac{\sum_{i=1}^N y_{ia}^{IA} - g_{IA}(\tilde{\alpha}_a^{(t)}) + \tilde{\alpha}_a^{(t)} h_{IA}(\tilde{\alpha}_a^{(t)})}{h_{IA}(\tilde{\alpha}_a^{(t)})}$$

, where $g_{IA}(\tilde{\alpha}_a^{(t)})$ is the partial derivative (gradient) of \mathbf{F}_{IA} with respect to $\tilde{\alpha}_a$, evaluated at $\tilde{\alpha}_a^{(t)}$; and $h_{IA}(\tilde{\alpha}_a^{(t)})$ is the second-order partial derivative of \mathbf{F}_{IA} with respect to $\tilde{\alpha}_a$, evaluated at $\tilde{\alpha}_a^{(t)}$.

5 Simulation Study

In this section, we conduct a simulation study to evaluate the performance of the proposed VBEM algorithm in terms of fitting the data and recovery of the link probabilities, model

parameters and latent positions.

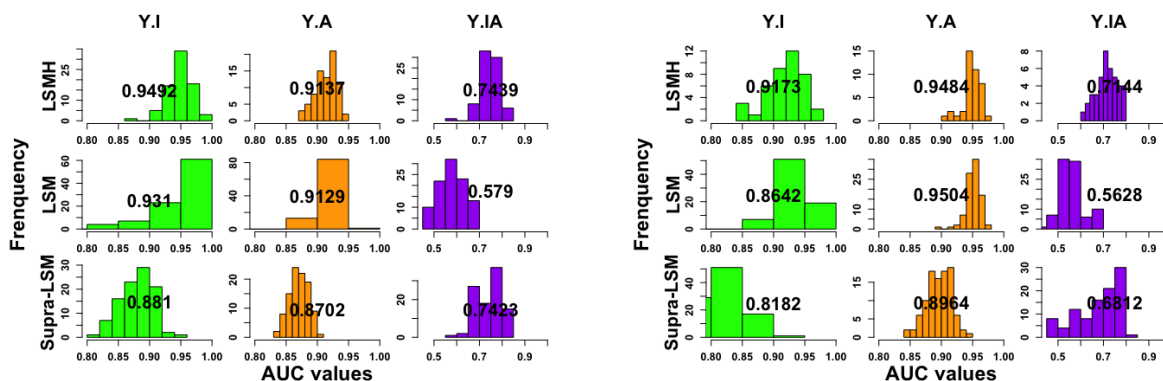


Figure 3: The histogram of AUC values for predicting Y_A, Y_I, Y_{IA} matrices over 100 simulations. Under the (left) first and (right) second settings, the α values are 1, .5, -0.5 and 3, 3.5, -2 respectively.

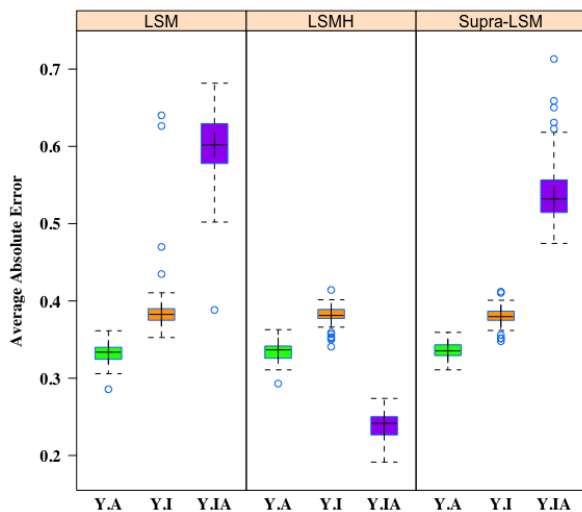


Figure 4: The boxplots of the average absolute error in estimating the true link probabilities in Y_I, Y_A, Y_{IA} matrices across 100 simulations. The α values are set to be 2, 1 and -2 respectively.

Our first assessment is in terms of the area under the receiver operating characteristic

curve (AUC) of predicting the presence or absence of a link from the estimated link probabilities. The LSMH defined by Equation 1 is our data generating model. The true values of λ_0, λ_1 are set to be 1 for this and all subsequent simulations. We sample \mathbf{Z}_I and \mathbf{Z}_A from the multivariate normal distributions using two sets of α parameter values: $\alpha_0 = 1, \alpha_1 = .5, \alpha_2 = -0.5$ and $\alpha_0 = 3, \alpha_1 = 3.5, \alpha_2 = -2$. Following Equation 1, we produce link probabilities between items, between persons and between items and persons using the inverse logistic link function. Next, we generated 100 datasets each consisting of the three matrices. Each element of the matrices (edge in the corresponding network) was generated from Bernoulli distribution using the corresponding link probability independent of all other elements. We apply the LSMH with the VBEM estimator to the simulated datasets and obtained the posterior distributions of the latent positions and estimates for the fixed parameters.

In Figure 3, we present the distributions of the AUC values for 100 simulations for $\mathbf{Y}_I, \mathbf{Y}_A$ and \mathbf{Y}_{IA} . To estimate the probability of an edge in $\mathbf{Y}_I, \mathbf{Y}_A$ and \mathbf{Y}_{IA} , we employ posterior means as point estimates of the latent positions following Equation 1. In the second and third rows of Figure 3, we compare the LSMH’s performance against two “baseline” procedures. For the first “baseline” procedure, we fit LSMs to \mathbf{Y}_I and \mathbf{Y}_A separately and calculated the link probability of an edge in \mathbf{Y}_{IA} . The LSMs are fitted using the variational inference method as described in [30]. Additionally, we apply a LSM to the item-person supra-adjacency matrix (a block matrix consisting of $\mathbf{Y}_I, \mathbf{Y}_A$ and \mathbf{Y}_{IA}) for the second “baseline” procedure. We refer to this method of applying the LSM as the supra-LSM. Contrary to our LSMH, the supra-LSM is fitted to $\mathbf{Y}_I, \mathbf{Y}_A$ and \mathbf{Y}_{IA} indiscriminately using a single α parameter and the same Euclidean distance measure across all three matrices. From Figure 3, we can see that the AUC values are higher using LSMH for \mathbf{Y}_I and \mathbf{Y}_A than those using supra-LSM, while the AUC values are higher using LSMH for \mathbf{Y}_{IA} than those using separate LSMs.

We can also compare the methods more directly in terms of the accuracy of estimating the link probabilities. In Figure 4, we present the average of the absolute differences between the known link probabilities and the estimated link probabilities, where the average is taken over all elements of the matrix under consideration, $\mathbf{Y}_I, \mathbf{Y}_A$ or \mathbf{Y}_{IA} . As can be seen, the AAEs are closer to 0 in the \mathbf{Y}_{IA} matrix using LSMH than those using the other two methods implying

a much better model fit to the data using LSMH. The performance of all the three methods are identical for the other two matrices.

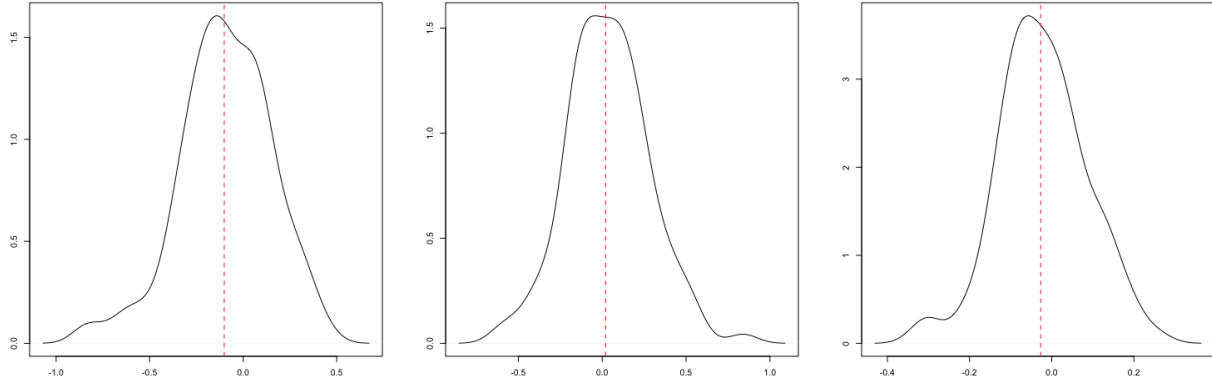


Figure 5: Results of 150 simulations. Distribution of the distance between the true and estimated α_0 (left), α_1 (middle) and α_2 (right) with different true α values.

5.0.1 Recovery of parameters and latent positions

We also assess the ability of the VBEM method in recovering the unknown model parameters and the latent positions of the nodes. In Figure 5, we present the distributions of distances between estimated values and the true values for α_0 , α_1 and α_2 respectively. We consider three sets of α values for this simulation, with 50 samples simulated for each set of α values for a total of 150 samples. Each density distribution in Figure 5 includes results from all the 150 simulations. The three sets of α values are $2, 2.5, -2$ and $2.5, 2, -1.5$ and $1.5, 2, -1$. The distribution of distances for each of $\alpha_0, \alpha_1, \alpha_2$ is narrow and centered roughly around 0, implying that the estimated α values are close to the true α values for a range of different true α values.

In Figure 6, we compare the pairwise distances from the estimated latent positions to those from the true latent positions similar to the comparison made in [68]. Even though the latent positions can be recovered only upto the ambiguity of an orthogonal transformation, the relative distances between nodes should be preserved. This implies the ratio of the distance between node i and j obtained using the estimates $\tilde{\mathbf{u}}_i$ and $\tilde{\mathbf{u}}_j$ and the true distance between node i and j obtained using true locations \mathbf{u}_i and \mathbf{u}_j should be close to 1 if the

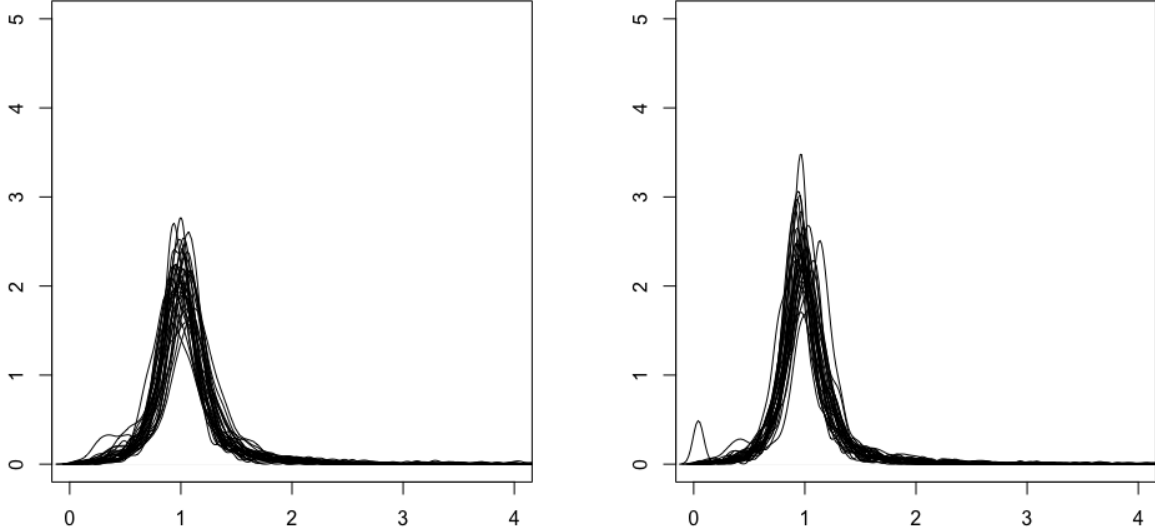


Figure 6: Distributions of pairwise distance ratios over 50 simulation samples, comparing $\tilde{\mathbf{u}}_i$ with \mathbf{u}_i (left) and $\tilde{\mathbf{v}}_a$ with \mathbf{v}_a (right) when α values are 2, 2.5, -2 .

VBEM estimation algorithm successfully maintained and recovered the relationship between node i and j . Therefore in Figure 6 we plot the distribution of this ratio for all pairs, where each plot is the distribution of this ratio for a pair of nodes over 50 samples. As can be seen in both plots in Figure 6, these distributions are narrow and centered around 1 for both sets of latent positions, implying successful recovery of the nodes’ relationships to each other through the estimated latent positions.

6 Analysis of the Early Learning Ohio Data

We applied LSMH to the data from each of the sixteen classrooms with $D = 2$ to study the relationship between friendship circles and students’ well-being in order to identify students with adjustment difficulties in each of these classrooms. We chose one of the classrooms, classroom 36, to illustrate in details the utility of LSMH, while results from 3 other classrooms are also presented in brief summaries. There were 28 students in classroom 36, 17 of which did not answer any item in the child interview questionnaire, and 7 of which did not report

their friendship information. Using the non-missing data we were able to obtain a 11×11 friendship matrix, \mathbf{Y}_I , and a 11×23 item response matrix, \mathbf{Y}_{IA} from classroom 36. The \mathbf{Y}_{IA} contained the dichotomized student responses, where both 1 and 2 responses are considered positive links between the students and the items.

We used the item relationship matrix \mathbf{Y}_A to include into our model the students' responses to the same items from other classrooms. In particular, the item relationship matrix was derived from the pairwise correlations of the 23 items measured over students across the remaining 15 classrooms. The \mathbf{Y}_A matrix then provides a source of information that is exogenous to or independent of the information from classroom 36. Including the item responses from the other classrooms in this way, we believe, will help solidify the positions of the items in relations to each other in the joint latent space. Items with strong positive correlations were considered to be connected in the item relationship matrix. We performed 253 one-tailed hypotheses tests ($H_0 : \rho \leq 0, H_a : \rho > 0$) on the pairwise Spearman's correlations [12] of the 23 items. The items were considered to be connected in \mathbf{Y}_A if their correlations were significantly positive with adjusted p values ($p \leq .005$). The p values were adjusted to control for multiple comparisons following [10]. In this way, the expected number of false positive connection is roughly one. The density of \mathbf{Y}_A is 0.2986767.

The results of LSMH from classroom 36 are shown in Figure 7 and Figure 10. We performed varimax rotation on the resulting latent item and person positions to improve the interpretability of the latent dimensions. The rotated latent positions of the items in the joint latent space can be seen in Figure 7. In the joint latent space, the items are colored according to the sub-scales they belong to. Similar to the PCA results, items from the same sub-scale are also found in similar directions. The second dimension of the joint latent space differentiates the NEA

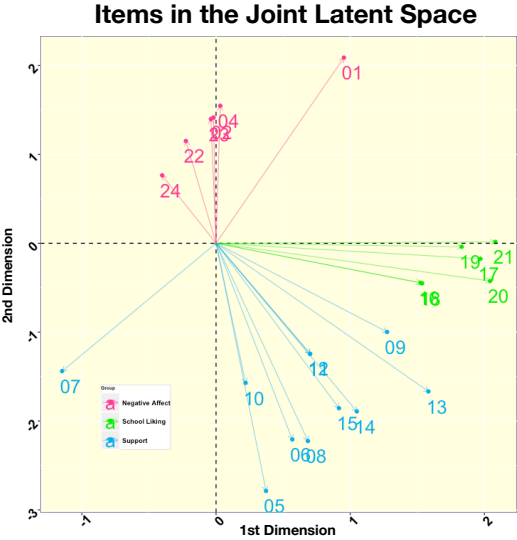


Figure 7: The positions of the items in the joint latent space. The items are colored according to their sub-scales.

items from the PSS items. This dimension is similar to the first dimension of the PCA and is interpreted as the NEA dimension.

The first dimension of the joint latent space has the same direction as the SL items and is interpreted as the SL dimension.

6.1 Joint versus Person Latent Space

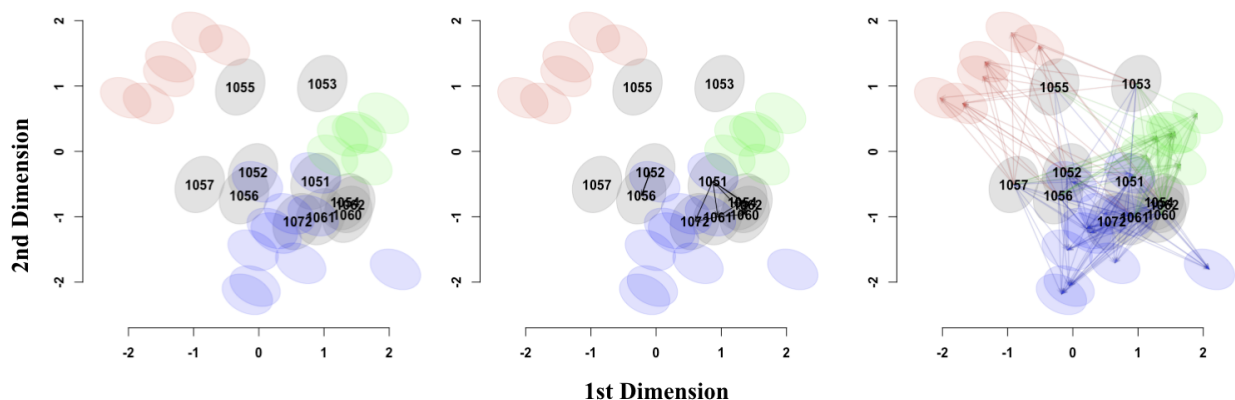


Figure 8: Latent positions $\tilde{\mathbf{u}}_i$ and $\tilde{\mathbf{v}}_a$ (left) with directed friendship edges (middle) and with directed item-response edges (right) for the joint modeling of the social network, the item relationship matrix and the item response matrix from classroom 36. The grey ellipses represent the 95% approximate credible intervals for the $\tilde{\mathbf{u}}_i$. The red, blue and green ellipses represent the 95% approximate credible intervals for the $\tilde{\mathbf{v}}_a$ in the NEA, PSS and SL sub-scale, respectively. The black edges represent the directed friendship edges after adjusting for missing data. The red, blue and green edges represent the students' positive responses to items under the NEA, PSS and SL sub-scales, respectively. The numbers are randomly assigned student identification numbers.

The estimated latent positions of the persons and items are shown in Figure 8 as well as in Figure 10. In Figure 8, we present the latent positions along with 95% approximate credible intervals. In addition, the middle and right plot in Figure 8 also contain the directed friendship edges and directed item-response edges respectively. In Figure 10, we present the

latent positions without the distraction of the edges. From Figure 8 to Figure 10, we will see that the information from the rather complex item-response edges is summarized through the latent positions of the students in relation to the latent positions of the items. More specifically, through an interpretation of the joint latent space, we are able to summarize students' response patterns, and thus assess their adjustment well-being.

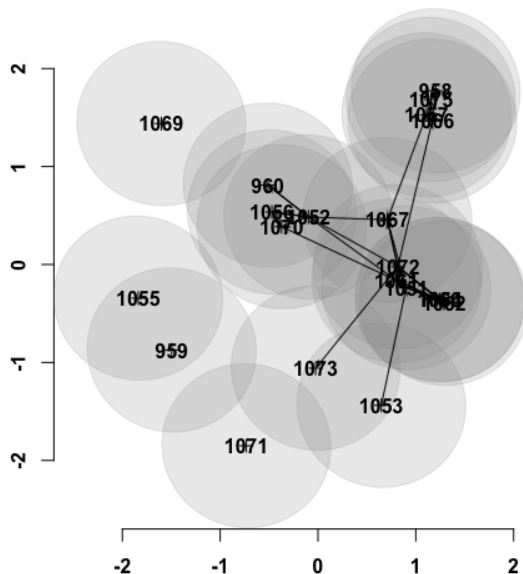


Figure 9: The latent positions of the students for the full social network in classroom 36 fitting the LSM. The directed arrows represent the directed friendship edges in the network.

To assess whether and how the latent person positions changed after adding students' survey responses, we applied the LSM to the students' full social network from classroom 36. This full latent person space can be found in the left panel of Figure 10. Due to 17 students' missing item responses, there are more students in the latent person space than in the joint latent space. Three major friendship clusters were observed using Euclidean distances, shown as the three purple circles. These friendship clusters were confirmed by the directed friendship edges in Figure 9. To help visually compare the joint latent space with person latent space, we also circled out the completely isolated students with red. These circles are not direct products of our model. We refer to the cluster in the lower right quadrant (away from the origin) as A , the cluster in the upper right quadrant (and close

to the origin) as B , and the cluster to the left of the origin as C . Students 1071, 1055, 959 and 1069 were positioned away from A , B and C , and therefore identified as isolated students. Students 1053 and 1073 are more isolated than the average of class 36 with only one friendship edge each.

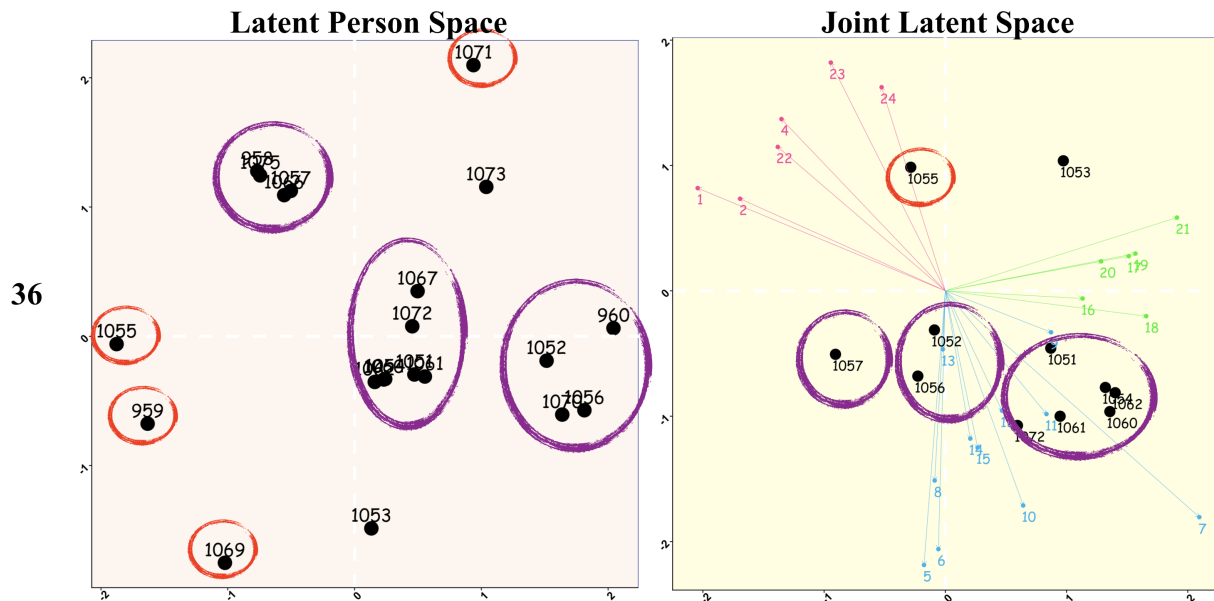


Figure 10: The latent positions of the students in the (left) latent person space and the (right) joint latent space

In the joint latent space in Figure 10, each student is shown as a black dot and is positioned following the predefined geometric rules. Euclidean distances are used to describe the person-person and item-item links. The smaller the Euclidean distance is between persons i and j , the more likely that person i and person j are friends; the smaller the Euclidean distance is between items a and b , the more likely that item a and item b measure similar adjustment attributes.

To interpret the links between item a and student i , we find [34]’s latent space project model as most fitting. The links between item a and student i are described with the dot product $\mathbf{u}_i^T \mathbf{v}_a$, which is the signed magnitude of the projection of \mathbf{u}_i in the direction of \mathbf{v}_a ($c_a \mathbf{w}_i^T \mathbf{w}_a$) multiplied by c_i resulting in $c_i c_a \mathbf{w}_i^T \mathbf{w}_a$. The magnitude of c_i captures student i ’s adjustment well-being, and magnitude of c_a captures the overall adjustment outcome

of students measured by item a . The angle between \mathbf{w}_i and \mathbf{w}_a captures the “similarity” between student i and item a . Together, $\mathbf{u}_i^T \mathbf{v}_a$ can be interpreted as the extent to which student i and item a share characteristics, multiplied by the well-being of student i and the adjustment outcome measured by item a . Items and the persons coexist and interact in the joint latent space through the shared adjustment information following the above geometric rules.

The positions of an item and a person are determined by the joint effect of how students in classroom 36 responded to different items, the student’s friendships with their peers and how similar the items are. By studying the positions of the students in relations to the items and other students, we can identify students with potential adjustment difficulties. For example, student 1055 seemed to be having a relatively difficult time. Student 1055 was positioned high on the NEA dimension and low on the SL dimension. Equivalently, the student was positioned at less-than-45-degree angles to the NEA items and at more-than-90-degree angles to the PPS and SL items. Meanwhile, most students in classroom 36 were positioned high on the SL dimension and low on the NEA dimension. Equivalently, they were positioned at more-than-90-degree angles to the NEA items and at less-than-45-degree angles to the PPS and SL items. This position of student 1055 compared to other students suggests that student 1055 had an opposite and unfavorable response pattern on the different items. More specifically, student 1055 scored high on the NEA items and low on the PSS and SL items while most students scored low on the NEA items and high on the PSS and SL items. In addition, student 1055 student was completely isolated in the latent person space. Taking both factors into account, we suspect that student 1055 was experiencing difficulties adjusting to school.

The results from the joint latent space show that students of the same friendship circle were more likely to have similar response patterns. In Figure 10, students of the friendship circle B (students 1051, 1054, 1060, 1061, 1062 and 1072) were positioned low on the NEA dimension, and high on the SL dimension. Students of A (students 1052, 1056) were positioned close to 0 on the NEA dimension and also on the SL dimension. Student 1057 of C were positioned close to 0 on the NEA dimension and very low on the SL dimension. In general, we can see that students who are close in Euclidean distances in the latent person

space are more likely to be at similar angles to different items (students’ responses to different items should always be interpreted following the vector products of $\tilde{\mathbf{u}}_i$ and $\tilde{\mathbf{v}}_a$) in the joint latent space. Using the joint latent space, we are able to find students’ with similar response patterns while taking into account of their friendship circles as shown in Table 1. As can be seen, students of the same friendship circles often reported similar sum scores of the items. This similarity in latent positions of students from the same friendship circle and dissimilarity of students from different friendship circles suggest that friends respond to different items similarly. It is unclear whether this similarity is a result of friendly connections or is the reason for friendship formation. The joint latent space allows us to observe this connection readily and distinctively. Future research should quantify and investigate further this connection between the friendship circle and the adjustment well-being.

Table 1: *Item sum scores for students in classroom 36*

PersonID	Negative Affect (NEA)	Support (PSS)	School Liking (SL)
1055	6	3	3
1053	4	5	6
1052	6	10	6
1056	3	9	6
1057	6	10	4
1051	2	11	6
1054	1	11	6
1060	0	11	6
1061	2	11	6
1062	1	11	6
1072	0	10	0
μ	2.818	9.273	5
sd	2.359	2.724	1.949

The joint latent space uniquely captures students’ individuality that is usually lost with traditional methods. Similar to students 1052 and 1056, student 1057 was also well socially supported. All three students were well-connected in the latent person space and positioned low in the NEA dimension. While students 1052 and 1056 were positioned neutral on the SL dimension, student 1057 was positioned in the opposite direction. Contrary to the common belief that well socially supported students have positive attitudes towards school, student 1057 had negative attitude towards school. This unusual perception of student 1057 was well

captured in the joint latent space and would have been lost under traditional methods. In particular, if we simply summarized students' friendship information with numbers of edges in the friendship network or if we simply summarized their item responses with sum scores of items, information regarding individual students such as student 1057 would have been lost. Using LSMH, we are able to capture distinctive variability at the individual node level.

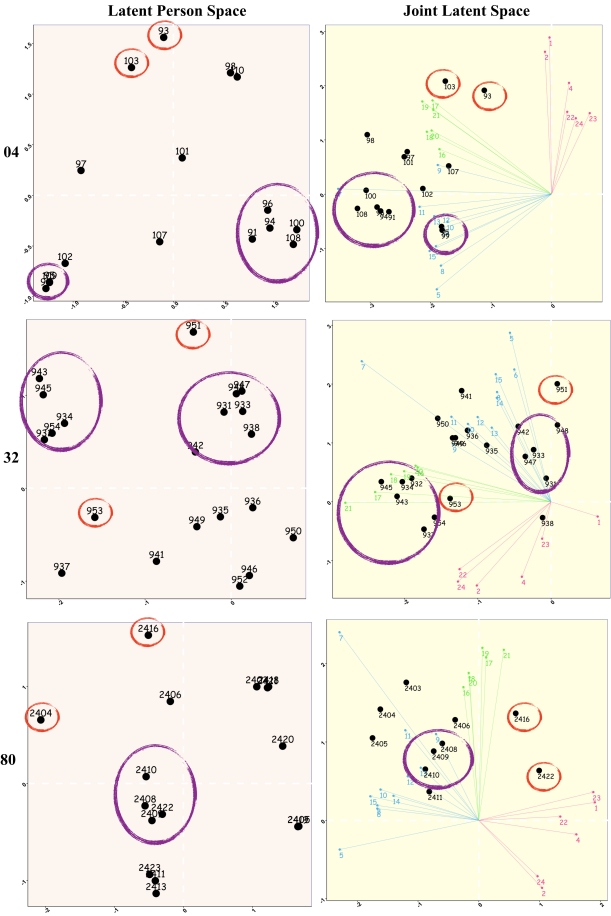


Figure 11: The person and joint latent spaces for classrooms (from top to bottom) 04, 32 and 80.

Students' experiences at school cannot be accurately reflected through their friendship circles alone. For example, students of *A* perceived less social support, felt more alone and encountered more negative experiences than those of *B* though students of friends group *A* and *B* were both all well-connected in the latent person space. This distinction in the well-being between students of *A* and *B* would not be readily observed through analyses of

only the friendship network. Another example can be found by comparing student 1055 and 1053. Student 1055 reported negative attitude towards school (low on the SL dimension) while student 1053 reported fairly positive attitude though both were isolated in the latent person space. Therefore, we are able to identify student 1055 as a potential candidate for intervention, but not student 1053. Only when we take into account both sources of information, can we obtain a more complete picture of a student’s well-being.

In Figure 11, we present the latent person and joint latent spaces from classrooms 04, 32 and 80 (top to the bottom). Students of the same friend groups, circled by purple, are often positioned in proximity to each other in the joint latent space. Isolated students, circled by red, are often positioned at smaller angles to the NEA items than the well-supported students. Though this connection between social support and students’ well-being is consistently observed, variations at the individual nodes (i.e., the individuality of students) can also be observed. For example, students 953 and 951 from classroom 32 are both identified as isolated in the person latent space. However, in the joint latent space, student 953 was positioned at less-than-90-degrees angle with the NEA items while student 951 was positioned at more-than-90-degrees angle with the NEA items. This shows that student 951 perceived negative experiences while student 953 did not though both were socially isolated. The latent person and joint latent spaces from the other 12 classrooms can be found in the Supplementary Material.

6.2 Model Fit

We assessed the fit of the LSMH to the data and compared it with the fit from fitting the LSMs to \mathbf{Y}_I and \mathbf{Y}_A separately and from fitting the supra-LSM to the supra-adjacency matrix. We present the Receiver Operating Characteristic (ROC) curves for predicting \mathbf{Y}_I , \mathbf{Y}_A and \mathbf{Y}_{IA} from classroom 36 in the left panel of Figure 12. From left to right, each column presents the ROC curve for \mathbf{Y}_I , \mathbf{Y}_A and \mathbf{Y}_{IA} matrices; from top to bottom, each row presents the ROC curves from fitting the LSMH, the LSMs separately and the supra-LSM.

The estimated $\tilde{\mathbf{u}}_i$ and $\tilde{\mathbf{v}}_a$ from fitting LSMs separately included information in \mathbf{Y}_I and \mathbf{Y}_A only. In comparison, the estimated $\tilde{\mathbf{u}}_i$ and $\tilde{\mathbf{v}}_a$ from fitting the LSMH included information in all three matrices. This difference in the $\tilde{\mathbf{u}}_i$ and $\tilde{\mathbf{v}}_a$ from fitting the LSMH versus fitting

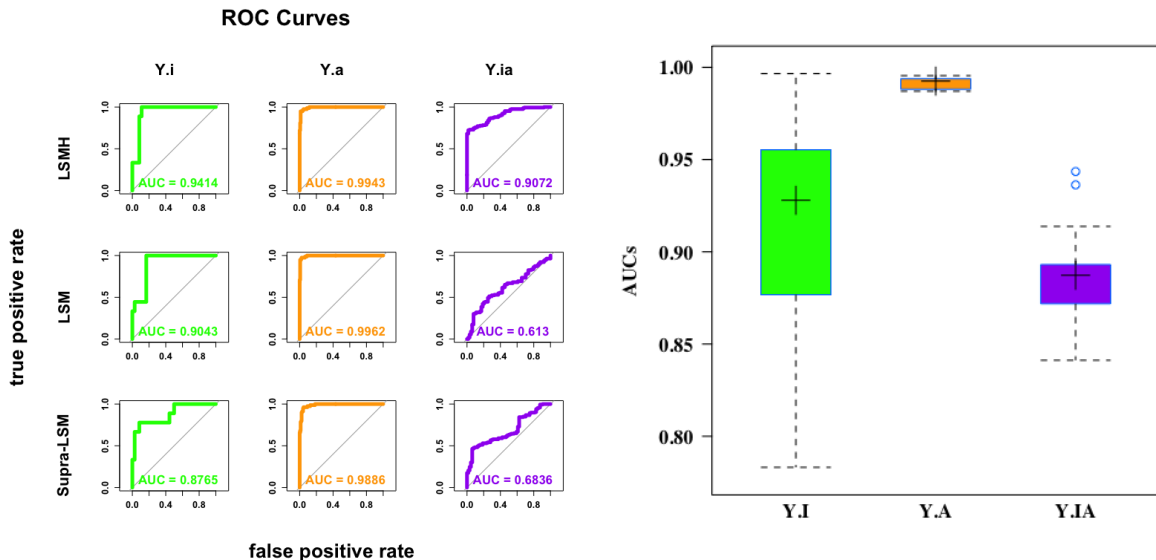


Figure 12: (A) Comparison of model fit to \mathbf{Y}_I , \mathbf{Y}_A and \mathbf{Y}_{IA} in terms of ROC curves among the LSMH, the LSM fitted separately to \mathbf{Y}_I and \mathbf{Y}_A and LSM fitted to the item-person supra-adjacency matrix (the supra-LSM) for classroom 36. (B) A boxplot describing the distribution of the AUC values on the three matrices over the 16 classrooms using LSMH

the LSMs separately is manifested through an increase in the AUC values from .613 to .9072 for \mathbf{Y}_{IA} and also an increase from .9043 to .9414 for \mathbf{Y}_I . The latter increase suggests that the $\tilde{\mathbf{u}}_i$ estimates were improved by including the information in \mathbf{Y}_A and \mathbf{Y}_{IA} resulting in an increase of fit for \mathbf{Y}_I . Overall, the results in Figure 12 show that the fit of the LSMH to the data is better than that of the separate LSMs and the supra-LSM as shown in our simulation.

In the right panel of Figure 12, we present the boxplot of AUC values from predicting the three matrices using LSMH across all 16 classrooms. As can be seen, LSMH fits the data from all classrooms well. In particular, LSMH fits \mathbf{Y}_A really well with the AUC values close to 1. The median of the AUC values for \mathbf{Y}_I is higher than that for \mathbf{Y}_{IA} ; the spread of the AUC values for \mathbf{Y}_I is also higher indicating greater variation in the fit for \mathbf{Y}_I across classrooms. Medians of the AUCs are close to 1 suggesting good model fit across all three matrices.

6.3 Prediction

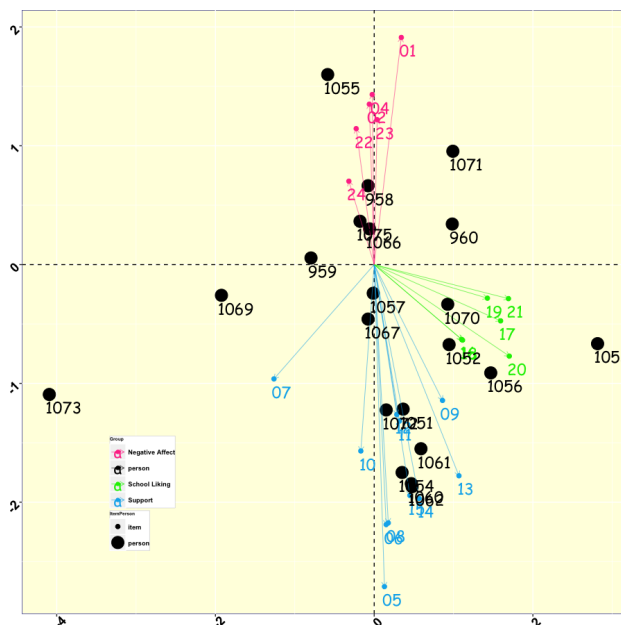


Figure 13: Predicted latent person positions of the missing students in classroom 36.

The LSMH can be used to predict missing (unobserved) links. We predicted the latent person positions of the 17 students from classroom 36 with missing item response information using their friendship information, their friends’ item responses and the item relationship matrix. The results can be seen in Figure 13. Using LSMH, students of the same friendship circles were predicted to have similar response patterns. For example, student 1070 was predicted to have similar response patterns as students 1052 and 1056. Students 958, 1066 and 1075 were predicted to have similar response patterns as student 1057. Isolated students (students 1071, 1069, 959) were predicted to respond high on the NEA items and low on the PSS and SL items.

6.4 LSMH-I

We applied the LSMH-I in Equation 2 with latent dimension $D = 2$ to the data from classroom 36. Using LSMH-I, we can obtain the multidimensional item discrimination and difficulty parameters taking into account the social network as well as the item responses.

We selected three representative items (item 1, 8 and 17), one from each sub-scale for an in-depth investigation. The difficulty and discrimination parameter estimates for the three items are shown in Table 2; the associated surface plots and contour plots are shown in Figure 14. The surface plot of an item is a plot, where the probability of a positive answer on this item is a function of students’ “abilities” in the D -dimensional space. The contour plot of an item contains equiprobability lines of the item, where the same probability of a positive answer can be expected for all students that fall on the line. In Figure 14, a red solid line indicates the direction of a equiprobability line. A red dashed line indicates the direction of the most rapid change in probabilities, which is also the direction the item has the most discriminating power. The length of the red dashed line indicates the discriminating power of the item. When the length is small, the item discriminates students’ of different adjustment well-being well. This discriminating power is summarized across the D dimensions by A_a s in Table 2.

Item	$z_{a,1}$	$z_{a,2}$	β_a	A_a	B_a
1	2.5006	-0.5066	-2.6128	2.5515	1.0241
8	-0.6927	-0.5154	0.4024	0.8634	-0.4661
17	-0.1679	2.1860	-2.6899	2.1924	1.2269

Table 2: *Item parameters and multidimensional statistics for the three test items*

From Figure 14, we can see that the three items discriminate different dimensions of students’ “abilities” and measure three different aspects of the school adjustment well-being. The red dashed line is almost parallel to the 1st dimension for item 1, almost parallel to the 2nd dimension for item 17, and is at 45 degree angle between the 1st and the 2nd dimension for item 8. This suggests that item 1 discriminates students of differing “abilities” in the 1st dimension best. Item 17 discriminates students of differing “abilities” in the 2nd dimension best. Item 8 discriminates students’ of differing “abilities” in both dimensions. The same conclusion can be drawn from the surface plots and the absolute values of $z_{a,1}$ and $z_{a,2}$ in

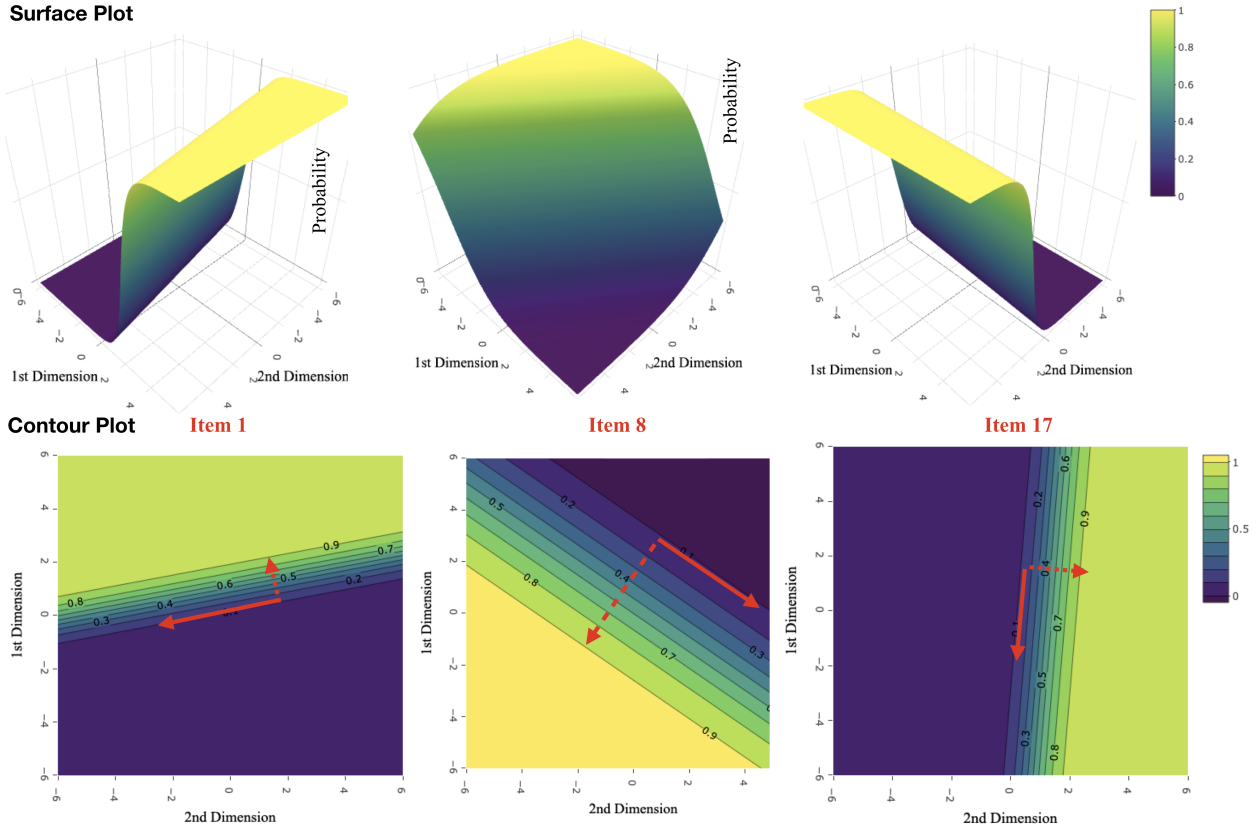


Figure 14: The surface plot and contour plot for the probability of positive response for items 1, 8 and 17

Table 2.

In Table 2, we summarize the difficulty information of item a across the D dimensions using B_a . In a contour plot, the absolute value of B_a is the distance between the .5 equiprobability line and the origin. A positive B_a suggests that the .5 equiprobability line is to the left of the origin and that the item is difficult. A negative B_a suggests that the .5 equiprobability line is to the right of the origin and that the item is easy. Among the three items in Table 2, items 1 and 17 are more difficult than item 8.

One can also aggregate item response data across classrooms for the purpose of studying the properties of the items using LSMH-I in Equation 3. However, since our primary goal is to understand students' adjustment well-being within a classroom, and not the assessment of the items, we do not investigate this direction further using the present dataset.

7 Discussions and conclusion

The LSMH outlined in this article constitutes a principle strategy for jointly analyzing social networks and item responses. We have argued for and presented evidence that a joint analysis of friendships and individual outcomes is crucial in understanding human behaviors. In particular, using LSMH, we analyzed the data from the Early Learning Ohio Project, identified the students with potential adjustment difficulties and found consistent connections between students' friendship circles and school adjustment well-being. We have shown that our joint analysis using LSMH provides more detailed information and more flexibility in analyzing the social and item-response network data than other currently available statistical models. Therefore, we believe that LSMH, as an exploratory analysis tool, can be used to greatly help researchers understand how friendships and item responses are intertwined and to inspire further model development in this area.

References

- [1] Agarwal, A. and Xue, L. [2019], 'Model-based clustering of nonparametric weighted networks with application to water pollution analysis', *Technometrics* (just-accepted), 1–25.
- [2] Airoldi, E. M., Blei, D. M., Fienberg, S. E. and Xing, E. P. [2008], 'Mixed membership stochastic blockmodels', *Journal of Machine Learning Research* **9**(Sep), 1981–2014.
- [3] Albert, R. and Barabási, A.-L. [2002], 'Statistical mechanics of complex networks', *Reviews of modern physics* **74**(1), 47.
- [4] Attias, H. [1999], Inferring parameters and structure of latent variable models by variational bayes, in 'Proceedings of the Fifteenth conference on Uncertainty in artificial intelligence', Morgan Kaufmann Publishers Inc., pp. 21–30.
- [5] Bagwell, C. L., Newcomb, A. F. and Bukowski, W. M. [1998], 'Preadolescent friendship and peer rejection as predictors of adult adjustment', *Child development* **69**(1), 140–153.
- [6] Barabási, A.-L. and Albert, R. [1999], 'Emergence of scaling in random networks', *science* **286**(5439), 509–512.
- [7] Baum, L. E., Petrie, T., Soules, G. and Weiss, N. [1970], 'A maximization technique occurring in the statistical analysis of probabilistic functions of markov chains', *The annals of mathematical statistics* **41**(1), 164–171.
- [8] Beal, M. J., Ghahramani, Z. et al. [2006], 'Variational bayesian learning of directed graphical models

- with hidden variables’, *Bayesian Analysis* **1**(4), 793–831.
- [9] Beal, M. J. et al. [2003], *Variational algorithms for approximate Bayesian inference*, university of London London.
- [10] Benjamini, Y. and Hochberg, Y. [1995], ‘Controlling the false discovery rate: a practical and powerful approach to multiple testing’, *Journal of the royal statistical society. Series B (Methodological)* pp. 289–300.
- [11] Berndt, T. J. and Keefe, K. [1995], ‘Friends’ influence on adolescents’ adjustment to school’, *Child development* **66**(5), 1312–1329.
- [12] Best, D. and Roberts, D. [1975], ‘Algorithm as 89: the upper tail probabilities of spearman’s rho’, *Journal of the Royal Statistical Society. Series C (Applied Statistics)* **24**(3), 377–379.
- [13] Bickel, P. J. and Chen, A. [2009], ‘A nonparametric view of network models and newman–girvan and other modularities’, *Proceedings of the National Academy of Sciences* **106**(50), 21068–21073.
- [14] Birch, S. H. and Ladd, G. W. [1997], ‘The teacher-child relationship and children’s early school adjustment’, *Journal of school psychology* **35**(1), 61–79.
- [15] Blei, D. M., Kucukelbir, A. and McAuliffe, J. D. [2017], ‘Variational inference: A review for statisticians’, *Journal of the American Statistical Association* **112**(518), 859–877.
- [16] Boccaletti, S., Bianconi, G., Criado, R., Del Genio, C. I., Gómez-Gardeñes, J., Romance, M., Sendina-Nadal, I., Wang, Z. and Zanin, M. [2014], ‘The structure and dynamics of multilayer networks’, *Physics Reports* **544**(1), 1–122.
- [17] Borsboom, D. and Cramer, A. O. [2013], ‘Network analysis: an integrative approach to the structure of psychopathology’, *Annual review of clinical psychology* **9**, 91–121.
- [18] Bullmore, E. and Sporns, O. [2009], ‘Complex brain networks: graph theoretical analysis of structural and functional systems’, *Nature Reviews Neuroscience* **10**(3), 186–198.
- [19] Celisse, A., Daudin, J. J. and Pierre, L. [2012], ‘Consistency of maximum-likelihood and variational estimators in the stochastic block model’, *Electronic Journal of Statistics* **6**, 1847–1899.
- [20] Daudin, J. J., Picard, F. and Robin, S. [2008], ‘A mixture model for random graphs’, *Stat Comput* **18**, 173–183.
- [21] Dean, D. O., Bauer, D. J. and Prinstein, M. J. [2017], ‘Friendship dissolution within social networks modeled through multilevel event history analysis’, *Multivariate behavioral research* **52**(3), 271–289.
- [22] Dempster, A. P., Laird, N. M. and Rubin, D. B. [1977], ‘Maximum likelihood from incomplete data via the em algorithm’, *Journal of the Royal Statistical Society. Series B (Methodological)* pp. 1–38.
- [23] Embretson, S. E. and Reise, S. P. [2000], ‘Item response theory for psychologists. maheah’.
- [24] Epskamp, S., Rhemtulla, M. and Borsboom, D. [2017], ‘Generalized network psychometrics: Combining network and latent variable models’, *Psychometrika* **82**(4), 904–927.
- [25] Erath, S. A., Flanagan, K. S. and Bierman, K. L. [2008], ‘Early adolescent school adjustment: Associations with friendship and peer victimization’, *Social Development* **17**(4), 853–870.

- [26] Ferrara, E., Interdonato, R. and Tagarelli, A. [2014], Online popularity and topical interests through the lens of instagram, *in* ‘Proceedings of the 25th ACM conference on Hypertext and social media’, ACM, pp. 24–34.
- [27] Fratiglioni, L., Wang, H.-X., Ericsson, K., Maytan, M. and Winblad, B. [2000], ‘Influence of social network on occurrence of dementia: a community-based longitudinal study’, *The lancet* **355**(9212), 1315–1319.
- [28] Friel, N., Rastelli, R., Wyse, J. and Raftery, A. E. [2016], ‘Interlocking directorates in irish companies using a latent space model for bipartite networks’, *Proceedings of the National Academy of Sciences* **113**(24), 6629–6634.
- [29] Girvan, M. and Newman, M. E. [2002], ‘Community structure in social and biological networks’, *Proceedings of the national academy of sciences* **99**(12), 7821–7826.
- [30] Gollini, I. and Murphy, T. B. [2016], ‘Joint modeling of multiple network views’, *Journal of Computational and Graphical Statistics* **25**(1), 246–265.
- [31] Handcock, M. S., Raftery, A. E. and Tantrum, J. M. [2007], ‘Model-based clustering for social networks’, *J. Roy. Statist. Soc. Ser. A* **170**, 301–354.
- [32] He, X., Kan, M.-Y., Xie, P. and Chen, X. [2014], Comment-based multi-view clustering of web 2.0 items, *in* ‘Proceedings of the 23rd international conference on World wide web’, ACM, pp. 771–782.
- [33] Henderson, H. V. and Searle, S. R. [1981], ‘On deriving the inverse of a sum of matrices’, *Siam Review* **23**(1), 53–60.
- [34] Hoff, P. D., Raftery, A. E. and Handcock, M. S. [2002], ‘Latent space approaches to social network analysis’, *Journal of the american Statistical association* **97**(460), 1090–1098.
- [35] Jackson, M. O. et al. [2008], *Social and economic networks*, Vol. 3, Princeton University Press Princeton.
- [36] Jensen, J. L. W. V. [1906], ‘Sur les fonctions convexes et les inégalités entre les valeurs moyennes’, *Acta mathematica* **30**(1), 175–193.
- [37] Jin, I. H. and Jeon, M. [2018], ‘A doubly latent space joint model for local item and person dependence in the analysis of item response data’, *Psychometrika* pp. 1–25.
- [38] Jordan, M. I., Ghahramani, Z., Jaakkola, T. S. and Saul, L. K. [1999], ‘An introduction to variational methods for graphical models’, *Machine learning* **37**(2), 183–233.
- [39] Kim, Y. and Srivastava, J. [2007], Impact of social influence in e-commerce decision making, *in* ‘Proceedings of the ninth international conference on Electronic commerce’, ACM, pp. 293–302.
- [40] Kindermann, T. A. [2007], ‘Effects of naturally existing peer groups on changes in academic engagement in a cohort of sixth graders’, *Child Development* **78**(4), 1186–1203.
- [41] Kingery, J. N., Erdley, C. A. and Marshall, K. C. [2011], ‘Peer acceptance and friendship as predictors of early adolescents’ adjustment across the middle school transition’, *Merrill-Palmer Quarterly (1982-)* pp. 215–243.
- [42] Kivelä, M., Arenas, A., Barthelemy, M., Gleeson, J. P., Moreno, Y. and Porter, M. A. [2014a], ‘Multi-

- layer networks’, *Journal of Complex Networks* **2**(3), 203–271.
- [43] Kivelä, M., Arenas, A., Barthelemy, M., Gleeson, J. P., Moreno, Y. and Porter, M. A. [2014*b*], ‘Multi-layer networks’, *Journal of complex networks* **2**(3), 203–271.
- [44] Krivitsky, P. N., Handcock, M. S., Raftery, A. E. and Hoff, P. D. [2009], ‘Representing degree distributions, clustering, and homophily in social networks with latent cluster random effects models’, *Social networks* **31**(3), 204–213.
- [45] Kwon, K. H., Stefanone, M. A. and Barnett, G. A. [2014], ‘Social network influence on online behavioral choices: exploring group formation on social network sites’, *American Behavioral Scientist* **58**(10), 1345–1360.
- [46] Ladd, G. W. and Kochenderfer, B. J. [1996], ‘Linkages between friendship and adjustment during early school transitions.’.
- [47] Ladd, G. W., Kochenderfer, B. J. and Coleman, C. C. [1996], ‘Friendship quality as a predictor of young children’s early school adjustment’, *Child development* **67**(3), 1103–1118.
- [48] Ladd, G. W., Kochenderfer, B. J. and Coleman, C. C. [1997], ‘Classroom peer acceptance, friendship, and victimization: Distinct relation systems that contribute uniquely to children’s school adjustment?’, *Child development* **68**(6), 1181–1197.
- [49] Liu, H., Jin, I. H. and Zhang, Z. [2018], ‘Structural equation modeling of social networks: Specification, estimation, and application’, *Multivariate behavioral research* pp. 1–17.
- [50] Liu, X., Liu, W., Murata, T. and Wakita, K. [2014], ‘A framework for community detection in heterogeneous multi-relational networks’, *Advances in Complex Systems* **17**(06), 1450018.
- [51] Marsman, M., Borsboom, D., Kruis, J., Epskamp, S., van Bork, R., Waldorp, L., Maas, H. v. d. and Maris, G. [2018], ‘An introduction to network psychometrics: Relating ising network models to item response theory models’, *Multivariate behavioral research* **53**(1), 15–35.
- [52] Matias, C. and Miele, V. [2016], ‘Statistical clustering of temporal networks through a dynamic stochastic block model’, *Journal of the Royal Statistical Society: Series B (Statistical Methodology)* .
- [53] McPherson, M., Smith-Lovin, L. and Cook, J. M. [2001], ‘Birds of a feather: Homophily in social networks’, *Annual review of sociology* **27**(1), 415–444.
- [54] Mellenbergh, G. J. [1994], ‘A unidimensional latent trait model for continuous item responses’, *Multivariate Behavioral Research* **29**(3), 223–236.
- [55] Mercken, L., Snijders, T. A., Steglich, C., Vartiainen, E. and De Vries, H. [2010], ‘Dynamics of adolescent friendship networks and smoking behavior’, *Social networks* **32**(1), 72–81.
- [56] Mucha, P. J., Richardson, T., Macon, K., Porter, M. A. and Onnela, J. P. [2010], ‘Community structure in time-dependent, multiscale, and multiplex networks’, *Science* **328**(5980), 876–878.
- [57] Nickel, M., Murphy, K., Tresp, V. and Gabrilovich, E. [2016], ‘A review of relational machine learning for knowledge graphs’, *Proceedings of the IEEE* **104**(1), 11–33.
- [58] Paul, S. and Chen, Y. [2016], ‘Consistent community detection in multi-relational data through re-

- stricted multi-layer stochastic blockmodel’, *Electronic Journal of Statistics* **10**(2), 3807–3870.
- [59] Paul, S. and Chen, Y. [2017], ‘Spectral and matrix factorization methods for consistent community detection in multi-layer networks’, *arXiv preprint arXiv:1704.07353* .
- [60] Rambaran, J. A., Hopmeyer, A., Schwartz, D., Steglich, C., Badaly, D. and Veenstra, R. [2017], ‘Academic functioning and peer influences: A short-term longitudinal study of network–behavior dynamics in middle adolescence’, *Child development* **88**(2), 523–543.
- [61] Reckase, M. D. [2009], Multidimensional item response theory models, in ‘Multidimensional Item Response Theory’, Springer, pp. 79–112.
- [62] Rubinov, M. and Sporns, O. [2010], ‘Complex network measures of brain connectivity: uses and interpretations’, *Neuroimage* **52**(3), 1059–1069.
- [63] Ryan, R. M. and Deci, E. L. [2000], ‘Self-determination theory and the facilitation of intrinsic motivation, social development, and well-being.’, *American psychologist* **55**(1), 68.
- [64] Salter-Townshend, M. and McCormick, T. H. [2017], ‘Latent space models for multiview network data’, *The annals of applied statistics* **11**(3), 1217.
- [65] Salter-Townshend, M. and Murphy, T. B. [2013], ‘Variational bayesian inference for the latent position cluster model for network data’, *Computational Statistics & Data Analysis* **57**(1), 661–671.
- [66] Schmittmann, V. D., Cramer, A. O., Waldorp, L. J., Epskamp, S., Kievit, R. A. and Borsboom, D. [2013], ‘Deconstructing the construct: A network perspective on psychological phenomena’, *New ideas in psychology* **31**(1), 43–53.
- [67] Sengupta, S. and Chen, Y. [2015], ‘Spectral clustering in heterogeneous networks’, *Statistica Sinica* pp. 1081–1106.
- [68] Sewell, D. K. and Chen, Y. [2015], ‘Latent space models for dynamic networks’, *Journal of the American Statistical Association* **110**(512), 1646–1657.
- [69] Sewell, D. K. and Chen, Y. [2016], ‘Latent space models for dynamic networks with weighted edges’, *Social Networks* **44**, 105–116.
- [70] Shin, H. and Ryan, A. M. [2014], ‘Early adolescent friendships and academic adjustment: Examining selection and influence processes with longitudinal social network analysis.’, *Developmental Psychology* **50**(11), 2462.
- [71] Shmulevich, I., Dougherty, E. R., Kim, S. and Zhang, W. [2002], ‘Probabilistic boolean networks: a rule-based uncertainty model for gene regulatory networks’, *Bioinformatics* **18**(2), 261–274.
- [72] Sun, Y., Yu, Y. and Han, J. [2009], Ranking-based clustering of heterogeneous information networks with star network schema, in ‘Proceedings of the 15th ACM SIGKDD international conference on Knowledge discovery and data mining’, ACM, pp. 797–806.
- [73] Van Der Linden, W. J. and Hambleton, R. K. [1997], Item response theory: Brief history, common models, and extensions, in ‘Handbook of modern item response theory’, Springer, pp. 1–28.
- [74] Watts, D. J. and Strogatz, S. H. [1998], ‘Collective dynamics of ‘small-world’ networks’, *nature*

393(6684), 440.

- [75] Wentzel, K. R., Barry, C. M. and Caldwell, K. A. [2004], ‘Friendships in middle school: Influences on motivation and school adjustment.’, *Journal of educational psychology* **96**(2), 195.
- [76] Xu, K. S., Kliger, M. and Hero Iii, A. O. [2014], ‘Adaptive evolutionary clustering’, *Data Mining and Knowledge Discovery* **28**(2), 304–336.
- [77] Zhao, Y., Levina, E. and Zhu, J. [2012], ‘Consistency of community detection in networks under degree-corrected stochastic block models’, *Ann. Statist* **40**, 2266–2292.

8 Supplementary materials

Supplementary Material for “Joint Analysis of Social and Item Response Networks with Latent Space Models”

Selena Shuo Wang, Subhadeep Paul, Jessica Logan and Paul De Boeck ¹

The Ohio State University

8.1 The Estimation Procedure for LSMH

8.1.1 Derivation of KL Divergence

We set the variational parameter as $\Theta = \tilde{\alpha}_0, \tilde{\alpha}_1, \tilde{\alpha}_2$ and $\tilde{\mathbf{u}}_i, \tilde{\Lambda}_0, \tilde{\mathbf{v}}_a, \tilde{\Lambda}_1$, where $q(\mathbf{u}_i) = N(\tilde{\mathbf{u}}_i, \tilde{\Lambda}_0)$, and $q(\mathbf{v}_a) = N(\tilde{\mathbf{v}}_a, \tilde{\Lambda}_1)$. We set the variational posterior as:

$$q(\mathbf{Z}_I, \mathbf{Z}_A | \mathbf{Y}_I, \mathbf{Y}_A, \mathbf{Y}_{IA}) = \prod_{i=1}^N q(\mathbf{u}_i) \prod_{a=1}^M q(\mathbf{v}_a)$$

The Kullback-Leiber divergence between the variational posterior and the true posterior is:

$$\begin{aligned} & \text{KL}[q(\mathbf{Z}_I, \mathbf{Z}_A, \alpha_0, \alpha_1, \alpha_2 | \mathbf{Y}_I, \mathbf{Y}_A, \mathbf{Y}_{IA}) | f(\mathbf{Z}_I, \mathbf{Z}_A, \alpha_0, \alpha_1, \alpha_2 | \mathbf{Y}_I, \mathbf{Y}_A, \mathbf{Y}_{IA})] \\ &= \int q(\mathbf{Z}_I, \mathbf{Z}_A, \alpha_0, \alpha_1, \alpha_2 | \mathbf{Y}_I, \mathbf{Y}_A, \mathbf{Y}_{IA}) \log \frac{q(\mathbf{Z}_I, \mathbf{Z}_A, \alpha_0, \alpha_1, \alpha_2 | \mathbf{Y}_I, \mathbf{Y}_A, \mathbf{Y}_{IA})}{f(\mathbf{Z}_I, \mathbf{Z}_A, \alpha_0, \alpha_1, \alpha_2 | \mathbf{Y}_I, \mathbf{Y}_A, \mathbf{Y}_{IA})} d(\mathbf{Z}_I, \mathbf{Z}_A, \alpha_0, \alpha_1, \alpha_2) \end{aligned}$$

¹E-mail: wang.10171@osu.edu, paul.963@osu.edu, logan.251@osu.edu, deboeck.02@osu.edu

$$\begin{aligned}
&= \int \prod_{i=1}^N q(\mathbf{u}_i) \prod_{a=1}^M q(\mathbf{v}_a) \log \frac{\prod_{i=1}^N q(\mathbf{u}_i) \prod_{a=1}^M q(\mathbf{v}_a)}{f(\mathbf{Y}_I, \mathbf{Y}_A, \mathbf{Y}_{IA} | \mathbf{Z}_I, \mathbf{Z}_A, \alpha_0, \alpha_1, \alpha_2) \prod_{i=1}^N f(\mathbf{u}_i) \prod_{a=1}^M f(\mathbf{v}_a)} d(\mathbf{Z}_I, \mathbf{Z}_A, \alpha_0, \alpha_1, \alpha_2) \\
&= \sum_{i=1}^N \int q(\mathbf{u}_i) \log \frac{q(\mathbf{u}_i)}{f(\mathbf{u}_i)} d\mathbf{u}_i + \sum_{a=1}^M \int q(\mathbf{v}_a) \log \frac{q(\mathbf{v}_a)}{f(\mathbf{v}_a)} d\mathbf{v}_a \\
&\quad - \int q(\mathbf{Z}_I, \mathbf{Z}_A, \alpha_0, \alpha_1, \alpha_2 | \mathbf{Y}_I, \mathbf{Y}_A, \mathbf{Y}_{IA}) \log f(\mathbf{Y}_I, \mathbf{Y}_A, \mathbf{Y}_{IA} | \mathbf{Z}_I, \mathbf{Z}_A, \alpha_0, \alpha_1, \alpha_2) d(\mathbf{Z}_I, \mathbf{Z}_A, \alpha_0, \alpha_1, \alpha_2) \\
&= \sum_{i=1}^N \text{KL}[q(\mathbf{u}_i) | f(\mathbf{u}_i)] + \sum_{a=1}^M \text{KL}[q(\mathbf{v}_a) | f(\mathbf{v}_a)] \\
&\quad - \mathbb{E}_{q(\mathbf{Z}_I, \mathbf{Z}_A, \alpha_0, \alpha_1, \alpha_2 | \mathbf{Y}_I, \mathbf{Y}_A, \mathbf{Y}_{IA})} [\log f(\mathbf{Y}_I, \mathbf{Y}_A, \mathbf{Y}_{IA} | \mathbf{Z}_I, \mathbf{Z}_A, \alpha_0, \alpha_1, \alpha_2)],
\end{aligned}$$

where each of the components are calculated as follows:

$$\begin{aligned}
&\sum_{i=1}^N \text{KL}[q(\mathbf{u}_i) | f(\mathbf{u}_i)] \\
&= - \sum_{i=1}^N \int q(\mathbf{u}_i) \log \frac{f(\mathbf{u}_i)}{q(\mathbf{u}_i)} d\mathbf{u}_i \\
&= - \sum_{i=1}^N \int q(\mathbf{u}_i) \left(\frac{1}{2} \left(-D \log(\lambda_0^2) + \log(\det(\tilde{\Lambda}_0)) - \frac{1}{\lambda_0^2} \mathbf{u}_i^T \mathbf{u}_i + (\mathbf{u}_i - \tilde{\mathbf{u}}_i)^T \tilde{\Lambda}_0^{-1} (\mathbf{u}_i - \tilde{\mathbf{u}}_i) \right) \right) \\
&= \frac{1}{2} \left(DN \log(\lambda_0^2) - N \log(\det(\tilde{\Lambda}_0)) \right) + \sum_{i=1}^N \frac{1}{2} \left(\frac{1}{\lambda_0^2} \mathbb{E}_{q(\mathbf{u}_i)} [\mathbf{u}_i^T \mathbf{u}_i] - \mathbb{E}_{q(\mathbf{u}_i)} [(\mathbf{u}_i - \tilde{\mathbf{u}}_i)^T \tilde{\Lambda}_0^{-1} (\mathbf{u}_i - \tilde{\mathbf{u}}_i)] \right) \\
&= \frac{1}{2} \left(DN \log(\lambda_0^2) - N \log(\det(\tilde{\Lambda}_0)) \right) + \sum_{i=1}^N \frac{1}{2\lambda_0^2} \left(\text{Var}(\mathbf{u}_i) + (\mathbb{E}_{q(\mathbf{u}_i)} [\mathbf{u}_i])^2 \right) - \frac{1}{2} ND \\
&= \frac{1}{2} \left(DN \log(\lambda_0^2) - N \log(\det(\tilde{\Lambda}_0)) \right) + \frac{N \text{tr}(\tilde{\Lambda}_0)}{2\lambda_0^2} + \frac{\sum_{i=1}^N \tilde{\mathbf{u}}_i^T \tilde{\mathbf{u}}_i}{2\lambda_0^2} - \frac{1}{2} ND \\
&\sum_{a=1}^M \text{KL}[q(\mathbf{v}_a) | f(\mathbf{v}_a)] \\
&= \frac{1}{2} \left(DM \log(\lambda_1^2) - M \log(\det(\tilde{\Lambda}_1)) \right) + \frac{M \text{tr}(\tilde{\Lambda}_1)}{2\lambda_1^2} + \frac{\sum_{a=1}^M \tilde{\mathbf{v}}_a^T \tilde{\mathbf{v}}_a}{2\lambda_1^2} - \frac{1}{2} MD
\end{aligned}$$

$\mathbb{E}_{q(\mathbf{Z}_I, \mathbf{Z}_A | \mathbf{Y}_I, \mathbf{Y}_A, \mathbf{Y}_{IA})} [\log f(\mathbf{Y}_I, \mathbf{Y}_A, \mathbf{Y}_{IA} | \mathbf{Z}_I, \mathbf{Z}_A)]$ can be expanded into 6 components:

$$\begin{aligned}
&\mathbb{E}_{q(\mathbf{Z}_I, \mathbf{Z}_A | \mathbf{Y}_I, \mathbf{Y}_A, \mathbf{Y}_{IA})} [\log f(\mathbf{Y}_I, \mathbf{Y}_A, \mathbf{Y}_{IA} | \mathbf{Z}_I, \mathbf{Z}_A)] \\
&= \sum_{i=1}^N \sum_{a=1}^M y_{ia} \mathbb{E}_{q(\mathbf{Z}_I, \mathbf{Z}_A | \mathbf{Y}_I, \mathbf{Y}_A, \mathbf{Y}_{IA})} [\alpha_2 + \mathbf{u}_i^T \mathbf{v}_a]
\end{aligned}$$

$$\begin{aligned}
& + \sum_{i=1}^N \sum_{j=1, j \neq i}^N y_{ij} \mathbb{E}_{q(\mathbf{Z}_I, \mathbf{Z}_A | \mathbf{Y}_I, \mathbf{Y}_A, \mathbf{Y}_{IA})} [\alpha_0 - (\mathbf{u}_i - \mathbf{u}_j)^T (\mathbf{u}_i - \mathbf{u}_j)] \\
& + \sum_{a=1}^M \sum_{b=1, b \neq a}^M y_{ab} \mathbb{E}_{q(\mathbf{Z}_I, \mathbf{Z}_A | \mathbf{Y}_I, \mathbf{Y}_A, \mathbf{Y}_{IA})} [\alpha_1 - (\mathbf{v}_a - \mathbf{v}_b)^T (\mathbf{v}_a - \mathbf{v}_b)] \\
& - \sum_{i=1}^N \sum_{a=1}^M \mathbb{E}_{q(\mathbf{Z}_I, \mathbf{Z}_A | \mathbf{Y}_I, \mathbf{Y}_A, \mathbf{Y}_{IA})} [\log(1 + \exp(\alpha_2 + \mathbf{u}_i^T \mathbf{v}_a))] \\
& - \sum_{i=1}^N \sum_{j=1, j \neq i}^N \mathbb{E}_{q(\mathbf{Z}_I, \mathbf{Z}_A | \mathbf{Y}_I, \mathbf{Y}_A, \mathbf{Y}_{IA})} [\log(1 + \exp(\alpha_0 - (\mathbf{u}_i - \mathbf{u}_j)^T (\mathbf{u}_i - \mathbf{u}_j))] \\
& - \sum_{a=1}^M \sum_{b=1, b \neq a}^M \mathbb{E}_{q(\mathbf{Z}_I, \mathbf{Z}_A | \mathbf{Y}_I, \mathbf{Y}_A, \mathbf{Y}_{IA})} [\log(1 + \exp(\alpha_1 - (\mathbf{v}_a - \mathbf{v}_b)^T (\mathbf{v}_a - \mathbf{v}_b))]
\end{aligned}$$

First 3 components of $\mathbb{E}_{q(\mathbf{Z}_I, \mathbf{Z}_A | \mathbf{Y}_I, \mathbf{Y}_A, \mathbf{Y}_{IA})} [\log f(\mathbf{Y}_I, \mathbf{Y}_A, \mathbf{Y}_{IA} | \mathbf{Z}_I, \mathbf{Z}_A)]$ are calculated as follows:

$$\begin{aligned}
& \sum_{i=1}^N \sum_{j=1, j \neq i}^N y_{ij} \mathbb{E}_{q(\mathbf{Z}_I, \mathbf{Z}_A | \mathbf{Y}_I, \mathbf{Y}_A, \mathbf{Y}_{IA})} [\alpha_0 - (\mathbf{u}_i - \mathbf{u}_j)^T (\mathbf{u}_i - \mathbf{u}_j)] \\
& = \sum_{i=1}^N \sum_{j=1, j \neq i}^N y_{ij} \int (\alpha_0 - (\mathbf{u}_i - \mathbf{u}_j)^T (\mathbf{u}_i - \mathbf{u}_j)) q(\mathbf{u}_i) q(\mathbf{u}_j) d(\mathbf{u}_i, \mathbf{u}_j) \\
& = \sum_{i=1}^N \sum_{j=1, j \neq i}^N y_{ij} \left[\tilde{\alpha}_0 - \int (\mathbf{u}_i - \mathbf{u}_j)^T (\mathbf{u}_i - \mathbf{u}_j) q(\mathbf{u}_i) q(\mathbf{u}_j) d(\mathbf{u}_i, \mathbf{u}_j) \right] \\
& = \sum_{i=1}^N \sum_{j=1, j \neq i}^N y_{ij} \left[\tilde{\alpha}_0 - \int \sum_{d=1}^D (u_{id} - u_{jd})^2 q(\mathbf{u}_i) q(\mathbf{u}_j) d(\mathbf{u}_i, \mathbf{u}_j) \right] \\
& = \sum_{i=1}^N \sum_{j=1, j \neq i}^N y_{ij} \left[\tilde{\alpha}_0 - \left[\sum_{d=1}^D \left[\int u_{id}^2 q(u_{id}) du_{id} + \int u_{jd}^2 q(u_{jd}) du_{jd} - \int \int 2u_{id} u_{jd} q(u_{id}) q(u_{jd}) du_{id}, du_{jd} \right] \right] \right] \\
& = \sum_{i=1}^N \sum_{j=1, j \neq i}^N y_{ij} \left[\tilde{\alpha}_0 - 2 \text{tr}(\tilde{\Lambda}_0) - (\tilde{\mathbf{u}}_i - \tilde{\mathbf{u}}_j)^T (\tilde{\mathbf{u}}_i - \tilde{\mathbf{u}}_j) \right] \\
& \sum_{a=1}^M \sum_{b=1, b \neq a}^M y_{ab} \mathbb{E}_{q(\mathbf{Z}_I, \mathbf{Z}_A | \mathbf{Y}_I, \mathbf{Y}_A, \mathbf{Y}_{IA})} [\alpha_1 - (\mathbf{v}_a - \mathbf{v}_b)^T (\mathbf{v}_a - \mathbf{v}_b)] \\
& = \sum_{a=1}^M \sum_{b=1, b \neq a}^M y_{ab} \left[\tilde{\alpha}_1 - 2 \text{tr}(\tilde{\Lambda}_1) - (\tilde{\mathbf{v}}_a - \tilde{\mathbf{v}}_b)^T (\tilde{\mathbf{v}}_a - \tilde{\mathbf{v}}_b) \right] \\
& \sum_{i=1}^N \sum_{a=1}^M y_{ia} \mathbb{E}_{q(\mathbf{Z}_I, \mathbf{Z}_A | \mathbf{Y}_I, \mathbf{Y}_A, \mathbf{Y}_{IA})} [\alpha_2 + \mathbf{u}_i^T \mathbf{v}_a]
\end{aligned}$$

$$= \sum_{i=1}^N \sum_{a=1}^M y_{ia} (\tilde{\alpha}_2 + \tilde{\mathbf{u}}_i^T \tilde{\mathbf{v}}_a)$$

The last 3 expectations of the log functions can be simplified using Jensen's inequality and $\mathbb{E}_{q(\mathbf{Z}_I, \mathbf{Z}_A | \mathbf{Y}_I, \mathbf{Y}_A, \mathbf{Y}_{IA})}[\log f(\mathbf{Y}_I, \mathbf{Y}_A, \mathbf{Y}_{IA} | \mathbf{Z}_I, \mathbf{Z}_A)]$ can be written as:

$$\begin{aligned} & \mathbb{E}_{q(\mathbf{Z}_I, \mathbf{Z}_A | \mathbf{Y}_I, \mathbf{Y}_A, \mathbf{Y}_{IA})}[\log f(\mathbf{Y}_I, \mathbf{Y}_A, \mathbf{Y}_{IA} | \mathbf{Z}_I, \mathbf{Z}_A)] \\ & \leq \sum_{i=1}^N \sum_{a=1}^M y_{ia} (\tilde{\alpha}_2 + \tilde{\mathbf{u}}_i^T \tilde{\mathbf{v}}_a) + \sum_{i=1}^N \sum_{j=1, j \neq i}^N y_{ij} \left[\tilde{\alpha}_0 - 2 \operatorname{tr}(\tilde{\Lambda}_0) - (\tilde{\mathbf{u}}_i - \tilde{\mathbf{u}}_j)^T (\tilde{\mathbf{u}}_i - \tilde{\mathbf{u}}_j) \right] \\ & \quad + \sum_{a=1}^M \sum_{b=1, b \neq a}^M y_{ab} \left[\tilde{\alpha}_1 - 2 \operatorname{tr}(\tilde{\Lambda}_1) - (\tilde{\mathbf{v}}_a - \tilde{\mathbf{v}}_b)^T (\tilde{\mathbf{v}}_a - \tilde{\mathbf{v}}_b) \right] \\ & \quad - \sum_{i=1}^N \sum_{a=1}^M \log(1 + \mathbb{E}_{q(\mathbf{Z}_I, \mathbf{Z}_A | \mathbf{Y}_I, \mathbf{Y}_A, \mathbf{Y}_{IA})}[\exp(\alpha_2 + \mathbf{u}_i^T \mathbf{v}_a)]) \\ & \quad - \sum_{i=1}^N \sum_{j=1, j \neq i}^N \log(1 + \mathbb{E}_{q(\mathbf{Z}_I, \mathbf{Z}_A | \mathbf{Y}_I, \mathbf{Y}_A, \mathbf{Y}_{IA})}[\exp(\alpha_0 - (\mathbf{u}_i - \mathbf{u}_j)^T (\mathbf{u}_i - \mathbf{u}_j))]) \\ & \quad - \sum_{a=1}^M \sum_{b=1, b \neq a}^M \log(1 + \mathbb{E}_{q(\mathbf{Z}_I, \mathbf{Z}_A | \mathbf{Y}_I, \mathbf{Y}_A, \mathbf{Y}_{IA})}[\exp(\alpha_1 - (\mathbf{v}_a - \mathbf{v}_b)^T (\mathbf{v}_a - \mathbf{v}_b))]) \end{aligned}$$

Recall $\mathbf{u}_i, \mathbf{u}_j$ are $D \times 1$ column vectors. Define $\mathbf{u} = \tilde{\mathbf{u}}_i - \tilde{\mathbf{u}}_j$. Then we have, $\mathbf{u}_i - \mathbf{u}_j \stackrel{iid}{=} N(\mathbf{u}, 2\tilde{\Lambda}_0)$, where \mathbf{u} is a $D \times 1$ vector and $\tilde{\Lambda}_0$ is an $n \times n$ positive semidefinite matrix. Further define $\mathbf{Z} = (2\tilde{\Lambda}_0)^{-1/2}(\mathbf{u}_i - \mathbf{u}_j - (\tilde{\mathbf{u}}_i - \tilde{\mathbf{u}}_j))$. Then clearly \mathbf{Z} follows D dimensional multivariate standard normal distribution and its density function is given by $f_{\mathbf{Z}}(z) = \frac{1}{\sqrt{2\pi}} \exp(-\frac{1}{2}\mathbf{z}^T \mathbf{z})$. Consequently, we have $\mathbf{u}_i - \mathbf{u}_j = 2\tilde{\Lambda}_0^{1/2} \mathbf{Z} + \mathbf{u}$.

Therefore, we can reparameterize

$$\begin{aligned} & \mathbb{E}_{q(\mathbf{Z}_I, \mathbf{Z}_A | \mathbf{Y}_I, \mathbf{Y}_A, \mathbf{Y}_{IA})}[\exp(-(\mathbf{u}_i - \mathbf{u}_j)^T (\mathbf{u}_i - \mathbf{u}_j))] \\ & = \mathbb{E}_{q(\mathbf{Z}_I, \mathbf{Z}_A | \mathbf{Y}_I, \mathbf{Y}_A, \mathbf{Y}_{IA})} \left[\exp \left(- \left(\mathbf{Z}^T (2\tilde{\Lambda}_0)^{1/2} + \mathbf{u}^T \right) \left((2\tilde{\Lambda}_0)^{1/2} \mathbf{Z} + \mathbf{u} \right) \right) \right] \\ & = \mathbb{E}_{q(\mathbf{Z}_I, \mathbf{Z}_A | \mathbf{Y}_I, \mathbf{Y}_A, \mathbf{Y}_{IA})} \left[\exp \left(- \mathbf{Z}^T (2\tilde{\Lambda}_0) \mathbf{Z} - 2\mathbf{Z}^T (2\tilde{\Lambda}_0)^{1/2} \mathbf{u} - \mathbf{u}^T \mathbf{u} \right) \right] \\ & = \frac{1}{\sqrt{2\pi}} \int \exp \left(- \mathbf{Z}^T (2\tilde{\Lambda}_0 + \frac{1}{2} \mathbf{I}) \mathbf{Z} - 2\mathbf{Z}^T (2\tilde{\Lambda}_0)^{1/2} \mathbf{u} - \mathbf{u}^T \mathbf{u} \right) d\mathbf{Z} \end{aligned}$$

Now define $Q = \mathbf{u}(2\tilde{\Lambda}_0 + \frac{1}{2}\mathbf{I})^{-1}(2\tilde{\Lambda}_0)^{1/2}$. Then the above integral becomes

$$\begin{aligned}
& \frac{1}{\sqrt{2\pi}} \int \exp \left(-(\mathbf{Z} - Q)^T (2\tilde{\Lambda}_0 + \frac{1}{2}\mathbf{I})(\mathbf{Z} - Q) - \mathbf{u}^T \mathbf{u} + \mathbf{u}^T (2\tilde{\Lambda}_0 + \frac{1}{2}\mathbf{I})^{-1} (2\tilde{\Lambda}_0) \mathbf{u} \right) d\mathbf{Z} \\
&= \exp \left(-\mathbf{u}^T \mathbf{u} + \mathbf{u}^T (2\tilde{\Lambda}_0 + \frac{1}{2}\mathbf{I})^{-1} (2\tilde{\Lambda}_0) \mathbf{u} \right) \det(\mathbf{I} + 4\tilde{\Lambda}_0)^{-\frac{1}{2}} \\
&= \exp \left(-\mathbf{u}^T (\mathbf{I} + (2\tilde{\Lambda}_0 + \frac{1}{2}\mathbf{I})^{-1} (2\tilde{\Lambda}_0)) \mathbf{u} \right) \det(\mathbf{I} + 4\tilde{\Lambda}_0)^{-\frac{1}{2}} \\
&= \exp \left(-\mathbf{u}^T (4\tilde{\Lambda}_0 + \mathbf{I})^{-1} \mathbf{u} \right) \det(\mathbf{I} + 4\tilde{\Lambda}_0)^{-\frac{1}{2}}.
\end{aligned}$$

The last line follows since for any two invertible matrices A and B , if $A+B$ is also invertible, then by [33]

$$(A + B)^{-1} = A^{-1} - A^{-1}B(I + A^{-1}B)^{-1}A^{-1}.$$

Letting $A = 4\tilde{\Lambda}_0$ and $B = I$ gives:

$$\mathbb{E}_{q(\mathbf{Z}_I, \mathbf{Z}_A | \mathbf{Y}_I, \mathbf{Y}_A, \mathbf{Y}_{IA})} [\exp(-(\mathbf{u}_i - \mathbf{u}_j)^T (\mathbf{u}_i - \mathbf{u}_j))] = \exp \left(-(\tilde{\mathbf{u}}_i - \tilde{\mathbf{u}}_j)^T (\mathbf{I} + 4\tilde{\Lambda}_0)^{-1} (\tilde{\mathbf{u}}_i - \tilde{\mathbf{u}}_j) \right) \det(\mathbf{I} + 4\tilde{\Lambda}_0)^{-\frac{1}{2}}$$

Following similar reparameterization, we find that

$$\mathbb{E}_{q(\mathbf{Z}_I, \mathbf{Z}_A | \mathbf{Y}_I, \mathbf{Y}_A, \mathbf{Y}_{IA})} [\exp(-(\mathbf{v}_a - \mathbf{v}_b)^T (\mathbf{v}_a - \mathbf{v}_b))] = \exp \left((\tilde{\mathbf{v}}_a - \tilde{\mathbf{v}}_b)^T (4\tilde{\Lambda}_1 + \mathbf{I})^{-1} (\tilde{\mathbf{v}}_a - \tilde{\mathbf{v}}_b) \right) \det(\mathbf{I} + 4\tilde{\Lambda}_1)^{-\frac{1}{2}}$$

Recall, \mathbf{Z} follows D dimensional multivariate standard normal distribution and its density function is given by $f_Z(z) = \frac{1}{\sqrt{2\pi}} \exp(-\frac{1}{2}\mathbf{z}^T \mathbf{z})$. Consequently, we have $\mathbf{u}_i^T = \mathbf{Z}^T \tilde{\Lambda}_0^{1/2} + \tilde{\mathbf{u}}_i^T$ and $\mathbf{v}_a = \tilde{\Lambda}_1^{1/2} \mathbf{Z} + \tilde{\mathbf{v}}_a$. Therefore, we can reparameterize

$$\begin{aligned}
& \mathbb{E}_{q(\mathbf{Z}_I, \mathbf{Z}_A | \mathbf{Y}_I, \mathbf{Y}_A, \mathbf{Y}_{IA})} [\exp(\mathbf{u}_i^T \mathbf{v}_a)] \\
&= \mathbb{E}_{q(\mathbf{Z}_I, \mathbf{Z}_A | \mathbf{Y}_I, \mathbf{Y}_A, \mathbf{Y}_{IA})} \left[\exp \left((\mathbf{Z}^T \tilde{\Lambda}_0^{1/2} + \tilde{\mathbf{u}}_i^T) (\tilde{\Lambda}_1^{1/2} \mathbf{Z} + \tilde{\mathbf{v}}_a) \right) \right] \\
&= \mathbb{E}_{q(\mathbf{Z}_I, \mathbf{Z}_A | \mathbf{Y}_I, \mathbf{Y}_A, \mathbf{Y}_{IA})} \left[\exp \left(\mathbf{Z}^T (\tilde{\Lambda}_0 \tilde{\Lambda}_1)^{1/2} \mathbf{Z} + \tilde{\mathbf{u}}_i^T \tilde{\Lambda}_1^{1/2} \mathbf{Z} + \tilde{\mathbf{v}}_a^T \tilde{\Lambda}_0^{1/2} \mathbf{Z} + \tilde{\mathbf{u}}_i^T \tilde{\mathbf{v}}_a \right) \right] \\
&= \frac{1}{\sqrt{2\pi}} \int \exp \left(\mathbf{Z}^T (\tilde{\Lambda}_0^{1/2} \tilde{\Lambda}_1^{1/2} - \frac{1}{2}\mathbf{I}) \mathbf{Z} + (\tilde{\mathbf{u}}_i^T \tilde{\Lambda}_1^{1/2} + \tilde{\mathbf{v}}_a^T \tilde{\Lambda}_0^{1/2}) \mathbf{Z} + \tilde{\mathbf{u}}_i^T \tilde{\mathbf{v}}_a \right) \\
&= \frac{1}{\sqrt{2\pi}} \int \exp \left(-\frac{1}{2} (\mathbf{Z} - Q)^T (\mathbf{I} - 2\tilde{\Lambda}_0^{1/2} \tilde{\Lambda}_1^{1/2}) (\mathbf{Z} - Q) + \tilde{\mathbf{u}}_i^T \tilde{\mathbf{v}}_a - Q^T (\tilde{\Lambda}_0^{1/2} \tilde{\Lambda}_1^{1/2} - \frac{1}{2}\mathbf{I}) Q \right) d(\mathbf{Z}), \\
& \left(Q^T = (\tilde{\mathbf{u}}_i^T \tilde{\Lambda}_1^{1/2} + \tilde{\mathbf{v}}_a^T \tilde{\Lambda}_0^{1/2}) (\mathbf{I} - 2\tilde{\Lambda}_0^{1/2} \tilde{\Lambda}_1^{1/2})^{-1} \right) \\
&= \exp \left(\tilde{\mathbf{u}}_i^T \tilde{\mathbf{v}}_a - Q^T (\tilde{\Lambda}_0^{1/2} \tilde{\Lambda}_1^{1/2} - \frac{1}{2}\mathbf{I}) Q \right) \det \left(\mathbf{I} - 2\tilde{\Lambda}_0^{1/2} \tilde{\Lambda}_1^{1/2} \right)^{-1/2}
\end{aligned}$$

$$= \det \left(\mathbf{I} - 2\tilde{\Lambda}_0^{1/2}\tilde{\Lambda}_1^{1/2} \right)^{-1/2} \exp \left(\tilde{\mathbf{u}}_i^T \tilde{\mathbf{v}}_a + \frac{1}{2} (\tilde{\Lambda}_1^{1/2} \tilde{\mathbf{u}}_i + \tilde{\Lambda}_0^{1/2} \tilde{\mathbf{v}}_a)^T (\mathbf{I} - 2\tilde{\Lambda}_1^{1/2}\tilde{\Lambda}_0^{1/2})^{-1} (\tilde{\Lambda}_1^{1/2} \tilde{\mathbf{u}}_i + \tilde{\Lambda}_0^{1/2} \tilde{\mathbf{v}}_a) \right)$$

Finally, the Kullback-Leiber divergence between the variational posterior and the true posterior is

$$\begin{aligned} & \text{KL}[q(\mathbf{Z}_I, \mathbf{Z}_A | \mathbf{Y}_I, \mathbf{Y}_A, \mathbf{Y}_{IA}) || f(\mathbf{Z}_I, \mathbf{Z}_A | \mathbf{Y}_I, \mathbf{Y}_A, \mathbf{Y}_{IA})] \\ & \geq \frac{1}{2} \left(DN \log(\lambda_0^2) - N \log(\det(\tilde{\Lambda}_0)) \right) + \frac{N \text{tr}(\tilde{\Lambda}_0)}{2\lambda_0^2} + \frac{\sum_{i=1}^N \tilde{\mathbf{u}}_i^T \tilde{\mathbf{u}}_i}{2\lambda_0^2} - \frac{1}{2} ND \\ & \quad + \frac{1}{2} \left(DM \log(\lambda_1^2) - M \log(\det(\tilde{\Lambda}_1)) \right) + \frac{M \text{tr}(\tilde{\Lambda}_1)}{2\lambda_1^2} + \frac{\sum_{a=1}^M \tilde{\mathbf{v}}_a^T \tilde{\mathbf{v}}_a}{2\lambda_1^2} - \frac{1}{2} MD \\ & \quad - \sum_{i=1}^N \sum_{a=1}^M y_{ia} (\tilde{\alpha}_2 + \tilde{\mathbf{u}}_i^T \tilde{\mathbf{v}}_a) - \sum_{i=1}^N \sum_{j=1, j \neq i}^N y_{ij} \left[\tilde{\alpha}_0 - 2 \text{tr}(\tilde{\Lambda}_0) - (\tilde{\mathbf{u}}_i - \tilde{\mathbf{u}}_j)^T (\tilde{\mathbf{u}}_i - \tilde{\mathbf{u}}_j) \right] \\ & \quad - \sum_{a=1}^M \sum_{b=1, b \neq a}^M y_{ab} \left[\tilde{\alpha}_1 - 2 \text{tr}(\tilde{\Lambda}_1) - (\tilde{\mathbf{v}}_a - \tilde{\mathbf{v}}_b)^T (\tilde{\mathbf{v}}_a - \tilde{\mathbf{v}}_b) \right] \\ & \quad + \sum_{i=1}^N \sum_{a=1}^M \log \left(1 + \frac{\exp(\tilde{\alpha}_2)}{\det \left(\mathbf{I} - 2\tilde{\Lambda}_0^{1/2}\tilde{\Lambda}_1^{1/2} \right)^{1/2}} \right. \\ & \quad \left. \exp \left(\tilde{\mathbf{u}}_i^T \tilde{\mathbf{v}}_a + \frac{1}{2} (\tilde{\Lambda}_1^{1/2} \tilde{\mathbf{u}}_i + \tilde{\Lambda}_0^{1/2} \tilde{\mathbf{v}}_a)^T (\mathbf{I} - 2\tilde{\Lambda}_1^{1/2}\tilde{\Lambda}_0^{1/2})^{-1} (\tilde{\Lambda}_1^{1/2} \tilde{\mathbf{u}}_i + \tilde{\Lambda}_0^{1/2} \tilde{\mathbf{v}}_a) \right) \right) \\ & \quad + \sum_{i=1}^N \sum_{j=1, j \neq i}^N \log \left(1 + \frac{\exp(\tilde{\alpha}_0)}{\det(\mathbf{I} + 4\tilde{\Lambda}_0)^{1/2}} \exp \left(- (\tilde{\mathbf{u}}_i - \tilde{\mathbf{u}}_j)^T (\mathbf{I} + 4\tilde{\Lambda}_0)^{-1} (\tilde{\mathbf{u}}_i - \tilde{\mathbf{u}}_j) \right) \right) \\ & \quad + \sum_{a=1}^M \sum_{b=1, b \neq a}^M \log \left(1 + \frac{\exp(\tilde{\alpha}_1)}{\det(\mathbf{I} + 4\tilde{\Lambda}_1)^{1/2}} \exp \left(- (\tilde{\mathbf{v}}_a - \tilde{\mathbf{v}}_b)^T (\mathbf{I} + 4\tilde{\Lambda}_1)^{-1} (\tilde{\mathbf{v}}_a - \tilde{\mathbf{v}}_b) \right) \right) \end{aligned}$$

8.1.2 Derivations of EM algorithms

E-step: Estimate $\tilde{\mathbf{u}}_i$, $\tilde{\mathbf{v}}_a$, $\tilde{\Lambda}_0$ and $\tilde{\Lambda}_1$ by minimizing the KL divergence.

$$\begin{aligned} & \text{KL}_{\tilde{\mathbf{u}}_i}[q(\mathbf{Z}_I, \mathbf{Z}_A | \mathbf{Y}_I, \mathbf{Y}_A, \mathbf{Y}_{IA}) || f(\mathbf{Z}_I, \mathbf{Z}_A | \mathbf{Y}_I, \mathbf{Y}_A, \mathbf{Y}_{IA})] \\ & \geq \frac{\sum_{i=1}^N \tilde{\mathbf{u}}_i^T \tilde{\mathbf{u}}_i}{2\lambda_0^2} - \sum_{i=1}^N \sum_{a=1}^M y_{ia} (\tilde{\alpha}_2 + \tilde{\mathbf{u}}_i^T \tilde{\mathbf{v}}_a) - \sum_{i=1}^N \sum_{j=1, j \neq i}^N y_{ij} \left[\tilde{\alpha}_0 - 2 \text{tr}(\tilde{\Lambda}_0) - (\tilde{\mathbf{u}}_i - \tilde{\mathbf{u}}_j)^T (\tilde{\mathbf{u}}_i - \tilde{\mathbf{u}}_j) \right] \\ & \quad + \sum_{i=1}^N \sum_{a=1}^M \log \left(1 + \frac{\exp(\tilde{\alpha}_2)}{\det \left(\mathbf{I} - 2\tilde{\Lambda}_0^{1/2}\tilde{\Lambda}_1^{1/2} \right)^{1/2}} \right) \end{aligned}$$

$$\begin{aligned} & \exp\left(\tilde{\mathbf{u}}_i^T \tilde{\mathbf{v}}_a + \frac{1}{2}(\tilde{\Lambda}_1^{1/2} \tilde{\mathbf{u}}_i + \tilde{\Lambda}_0^{1/2} \tilde{\mathbf{v}}_a)^T (\mathbf{I} - 2\tilde{\Lambda}_1^{1/2} \tilde{\Lambda}_0^{1/2})^{-1} (\tilde{\Lambda}_1^{1/2} \tilde{\mathbf{u}}_i + \tilde{\Lambda}_0^{1/2} \tilde{\mathbf{v}}_a)\right) \\ & + \sum_{i=1}^N \sum_{j=1, j \neq i}^N \log\left(1 + \frac{\exp(\tilde{\alpha}_0)}{\det(\mathbf{I} + 4\tilde{\Lambda}_0)^{1/2}} \exp\left(-(\tilde{\mathbf{u}}_i - \tilde{\mathbf{u}}_j)^T (\mathbf{I} + 4\tilde{\Lambda}_0)^{-1} (\tilde{\mathbf{u}}_i - \tilde{\mathbf{u}}_j)\right)\right) + \text{Const} \tilde{\mathbf{u}}_i \end{aligned}$$

To find the closed form updates of $\tilde{\mathbf{u}}_i$, we use second-order Taylor-expansions of

$$\begin{aligned} \mathbf{F}_{ia} = \sum_{i=1}^N \sum_{a=1}^M \log\left(1 + \frac{\exp(\tilde{\alpha}_2)}{\det(\mathbf{I} - 2\tilde{\Lambda}_0^{1/2} \tilde{\Lambda}_1^{1/2})^{1/2}} \right. \\ \left. \exp\left(\tilde{\mathbf{u}}_i^T \tilde{\mathbf{v}}_a + \frac{1}{2}(\tilde{\Lambda}_1^{1/2} \tilde{\mathbf{u}}_i + \tilde{\Lambda}_0^{1/2} \tilde{\mathbf{v}}_a)^T (\mathbf{I} - 2\tilde{\Lambda}_0^{1/2} \tilde{\Lambda}_1^{1/2})^{-1} (\tilde{\Lambda}_1^{1/2} \tilde{\mathbf{u}}_i + \tilde{\Lambda}_0^{1/2} \tilde{\mathbf{v}}_a)\right)\right) \end{aligned} \quad (4)$$

$$\mathbf{F}_i = \sum_{i=1}^N \sum_{j=1, j \neq i}^N \log\left(1 + \frac{\exp(\tilde{\alpha}_0)}{\det(\mathbf{I} + 4\tilde{\Lambda}_0)^{1/2}} \exp\left(-(\tilde{\mathbf{u}}_i - \tilde{\mathbf{u}}_j)^T (\mathbf{I} + 4\tilde{\Lambda}_0)^{-1} (\tilde{\mathbf{u}}_i - \tilde{\mathbf{u}}_j)\right)\right) \quad (5)$$

To simplify the forms, we denote $(\mathbf{I} - 2\tilde{\Lambda}_0^{1/2} \tilde{\Lambda}_1^{1/2})^{-1}$ as \mathbf{B} . The gradients of \mathbf{F}_i and \mathbf{F}_{ia} with respect to $\tilde{\mathbf{u}}_i$ are

$$\begin{aligned} \mathbf{G}_i(\tilde{\mathbf{u}}_i) &= -2(\mathbf{I} + 4\tilde{\Lambda}_0)^{-1} \sum_{j=1, j \neq i}^N (\tilde{\mathbf{u}}_i - \tilde{\mathbf{u}}_j) \left[1 + \frac{\det(\mathbf{I} + 4\tilde{\Lambda}_0)^{1/2}}{\exp(\tilde{\alpha}_0)} \exp\left((\tilde{\mathbf{u}}_i - \tilde{\mathbf{u}}_j)^T (\mathbf{I} + 4\tilde{\Lambda}_0)^{-1} (\tilde{\mathbf{u}}_i - \tilde{\mathbf{u}}_j)\right)\right]^{-1} \\ \mathbf{G}_{ia}(\tilde{\mathbf{u}}_i) &= \sum_{a=1}^M \left(\left(.5\tilde{\Lambda}_1^{1/2} (\mathbf{B} + \mathbf{B}^T) \tilde{\Lambda}_0^{1/2} + \mathbf{I} \right) \tilde{\mathbf{v}}_a + .5\tilde{\Lambda}_1^{1/2} (\mathbf{B} + \mathbf{B}^T) \tilde{\Lambda}_1^{1/2} \tilde{\mathbf{u}}_i \right) \\ & \left[1 + \frac{\det(\mathbf{I} - 2\tilde{\Lambda}_1^{1/2} \tilde{\Lambda}_0^{1/2})^{1/2}}{\exp(\tilde{\alpha}_2)} \exp\left(-\tilde{\mathbf{u}}_i^T \tilde{\mathbf{v}}_a - \frac{1}{2}(\tilde{\Lambda}_1^{1/2} \tilde{\mathbf{u}}_i + \tilde{\Lambda}_0^{1/2} \tilde{\mathbf{v}}_a)^T \mathbf{B}^T (\tilde{\Lambda}_1^{1/2} \tilde{\mathbf{u}}_i + \tilde{\Lambda}_0^{1/2} \tilde{\mathbf{v}}_a)\right)\right]^{-1} \end{aligned}$$

The second-order partial derivatives (Hessian matrices) of $\mathbf{F}_i, \mathbf{F}_{ia}$ with respect to $\tilde{\mathbf{u}}_i$ are

$$\begin{aligned} \mathbf{H}_i(\tilde{\mathbf{u}}_i) &= -2(\mathbf{I} + 4\tilde{\Lambda}_0)^{-1} \sum_{j=1, j \neq i}^N \left[1 + \frac{\det(\mathbf{I} + 4\tilde{\Lambda}_0)^{1/2}}{\exp(\tilde{\alpha}_0)} \exp\left((\tilde{\mathbf{u}}_i - \tilde{\mathbf{u}}_j)^T (\mathbf{I} + 4\tilde{\Lambda}_0)^{-1} (\tilde{\mathbf{u}}_i - \tilde{\mathbf{u}}_j)\right)\right]^{-1} \\ & \left[\mathbf{I} - \frac{2(\tilde{\mathbf{u}}_i - \tilde{\mathbf{u}}_j)(\tilde{\mathbf{u}}_i - \tilde{\mathbf{u}}_j)^T (\mathbf{I} + 4\tilde{\Lambda}_0)^{-1}}{1 + \frac{\exp(\tilde{\alpha}_0)}{\det(\mathbf{I} + 4\tilde{\Lambda}_0)^{1/2}} \exp\left(-(\tilde{\mathbf{u}}_i - \tilde{\mathbf{u}}_j)^T (\mathbf{I} + 4\tilde{\Lambda}_0)^{-1} (\tilde{\mathbf{u}}_i - \tilde{\mathbf{u}}_j)\right)} \right] \\ \mathbf{H}_{ia}(\tilde{\mathbf{u}}_i) &= \sum_{a=1}^M \left[1 + \frac{\det(\mathbf{I} - 2\tilde{\Lambda}_1^{1/2} \tilde{\Lambda}_0^{1/2})^{1/2}}{\exp(\tilde{\alpha}_2)} \exp\left(-\tilde{\mathbf{u}}_i^T \tilde{\mathbf{v}}_a - \frac{1}{2}(\tilde{\Lambda}_1^{1/2} \tilde{\mathbf{u}}_i + \tilde{\Lambda}_0^{1/2} \tilde{\mathbf{v}}_a)^T \mathbf{B}^T (\tilde{\Lambda}_1^{1/2} \tilde{\mathbf{u}}_i + \tilde{\Lambda}_0^{1/2} \tilde{\mathbf{v}}_a)\right)\right]^{-1} \end{aligned}$$

$$\left[\tilde{\Lambda}_1^{1/2} B \tilde{\Lambda}_1^{1/2} + \frac{\left(\left(.5 \tilde{\Lambda}_1^{1/2} B \tilde{\Lambda}_0^{1/2} + \mathbf{I} \right) \tilde{\mathbf{v}}_a + .5 \tilde{\Lambda}_1^{1/2} B \tilde{\Lambda}_1^{1/2} \tilde{\mathbf{u}}_i \right) \left(\left(.5 \tilde{\Lambda}_1^{1/2} B \tilde{\Lambda}_0^{1/2} + \mathbf{I} \right) \tilde{\mathbf{v}}_a + .5 \tilde{\Lambda}_1^{1/2} B \tilde{\Lambda}_1^{1/2} \tilde{\mathbf{u}}_i \right)^T}{1 + \frac{\exp(\tilde{\alpha}_2)}{\det(\mathbf{I} - 2\tilde{\Lambda}_1^{1/2} \tilde{\Lambda}_0^{1/2})^{1/2}} \exp\left(\tilde{\mathbf{u}}_i^T \tilde{\mathbf{v}}_a + \frac{1}{2}(\tilde{\Lambda}_1^{1/2} \tilde{\mathbf{u}}_i + \tilde{\Lambda}_0^{1/2} \tilde{\mathbf{v}}_a)^T B^T (\tilde{\Lambda}_1^{1/2} \tilde{\mathbf{u}}_i + \tilde{\Lambda}_0^{1/2} \tilde{\mathbf{v}}_a)\right)} \right]^T$$

With the Taylor-expansions of the log functions, we can obtain the closed form update rule of $\tilde{\mathbf{u}}_i$ by setting the partial derivative of KL equal to 0. Finally, we have

$$\tilde{\mathbf{u}}_i = \left[\left(\frac{1}{2\lambda_0} + \sum_{j=1, j \neq i}^N (y_{ji} + y_{ij}) \right) \mathbf{I} + \mathbf{H}_i(\tilde{\mathbf{u}}_i) + \frac{1}{2} \mathbf{H}_{ia}(\tilde{\mathbf{u}}_i) \right]^{-1} \left[\sum_{j=1, j \neq i}^N (y_{ji} + y_{ij}) \tilde{\mathbf{u}}_j + \frac{1}{2} \sum_{a=1}^M y_{ia} \tilde{\mathbf{v}}_a - \mathbf{G}_i(\tilde{\mathbf{u}}_i) + \left(\mathbf{H}_i(\tilde{\mathbf{u}}_i) + \frac{1}{2} \mathbf{H}_{ia}(\tilde{\mathbf{u}}_i) \right) \tilde{\mathbf{u}}_i - \frac{1}{2} \mathbf{G}_{ia}(\tilde{\mathbf{u}}_i) \right]$$

$$\tilde{\mathbf{v}}_a = \left[\left(\frac{1}{2\lambda_1} + \sum_{b=1, b \neq a}^M (y_{ba} + y_{ab}) \right) \mathbf{I} + \mathbf{H}_a(\tilde{\mathbf{v}}_a) + \frac{1}{2} \mathbf{H}_{ia}(\tilde{\mathbf{v}}_a) \right]^{-1} \left[\sum_{b=1, b \neq a}^M (y_{ba} + y_{ab}) \tilde{\mathbf{v}}_b + \frac{1}{2} \sum_{i=1}^N y_{ia} \tilde{\mathbf{u}}_i - \mathbf{G}_a(\tilde{\mathbf{v}}_a) + \left(\mathbf{H}_a(\tilde{\mathbf{v}}_a) + \frac{1}{2} \mathbf{H}_{ia}(\tilde{\mathbf{v}}_a) \right) \tilde{\mathbf{v}}_a - \frac{1}{2} \mathbf{G}_{ia}(\tilde{\mathbf{v}}_a) \right]$$

Similarly, we can obtain the closed form update rule for $\tilde{\mathbf{v}}_a$ by taking the second order Taylor-expansion of \mathbf{F}_a and \mathbf{F}_{ia} (see Equation 4)

$$\mathbf{F}_a = \sum_{a=1}^M \sum_{b=1, b \neq a}^M \log \left(1 + \frac{\exp(\tilde{\alpha}_1)}{\det(\mathbf{I} + 4\tilde{\Lambda}_1)^{1/2}} \exp \left(-(\tilde{\mathbf{v}}_a - \tilde{\mathbf{v}}_b)^T (\mathbf{I} + 4\tilde{\Lambda}_1)^{-1} (\tilde{\mathbf{v}}_a - \tilde{\mathbf{v}}_b) \right) \right)$$

The gradients of $\mathbf{F}_a, \mathbf{F}_{ia}$ with respect to $\tilde{\mathbf{v}}_a$ are

$$\mathbf{G}_a(\tilde{\mathbf{v}}_a) = -2(\mathbf{I} + 4\tilde{\Lambda}_1)^{-1} \sum_{b=1, b \neq a}^M (\tilde{\mathbf{v}}_a - \tilde{\mathbf{v}}_b) \left[1 + \frac{\det(\mathbf{I} + 4\tilde{\Lambda}_1)^{1/2}}{\exp(\tilde{\alpha}_1)} \exp \left((\tilde{\mathbf{v}}_a - \tilde{\mathbf{v}}_b)^T (\mathbf{I} + 4\tilde{\Lambda}_1)^{-1} (\tilde{\mathbf{v}}_a - \tilde{\mathbf{v}}_b) \right) \right]^{-1}$$

$$\mathbf{G}_{ia}(\tilde{\mathbf{v}}_a) = \sum_{i=1}^N \left(\left(.5 \tilde{\Lambda}_0^{1/2} (B + B^T) \tilde{\Lambda}_1^{1/2} + \mathbf{I} \right) \tilde{\mathbf{u}}_i + .5 \Lambda_0^{1/2} (B + B^T) \Lambda_0^{1/2} \tilde{\mathbf{v}}_a \right) \left[1 + \frac{\det(\mathbf{I} - 2\tilde{\Lambda}_1^{1/2} \tilde{\Lambda}_0^{1/2})^{1/2}}{\exp(\tilde{\alpha}_2)} \exp \left(-\tilde{\mathbf{u}}_i^T \tilde{\mathbf{v}}_a - \frac{1}{2} (\tilde{\Lambda}_1^{1/2} \tilde{\mathbf{u}}_i + \tilde{\Lambda}_0^{1/2} \tilde{\mathbf{v}}_a)^T B^T (\tilde{\Lambda}_1^{1/2} \tilde{\mathbf{u}}_i + \tilde{\Lambda}_0^{1/2} \tilde{\mathbf{v}}_a) \right) \right]^{-1}$$

Hessian matrices of \mathbf{F}_a and \mathbf{F}_{ia} with respect to $\tilde{\mathbf{v}}_a$ are

$$\mathbf{H}_a(\tilde{\mathbf{v}}_a) = -2(\mathbf{I} + 4\tilde{\Lambda}_1)^{-1} \sum_{b=1, b \neq a}^M (\tilde{\mathbf{v}}_a - \tilde{\mathbf{v}}_b) \left[1 + \frac{\det(\mathbf{I} + 4\tilde{\Lambda}_1)^{1/2}}{\exp(\tilde{\alpha}_1)} \exp \left((\tilde{\mathbf{v}}_a - \tilde{\mathbf{v}}_b)^T (\mathbf{I} + 4\tilde{\Lambda}_1)^{-1} (\tilde{\mathbf{v}}_a - \tilde{\mathbf{v}}_b) \right) \right]^{-1}$$

$$\left[\mathbf{I} - \frac{2(\tilde{\mathbf{v}}_a - \tilde{\mathbf{v}}_b)(\tilde{\mathbf{v}}_a - \tilde{\mathbf{v}}_b)^T (\mathbf{I} + 4\tilde{\Lambda}_1)^{-1}}{1 + \frac{\exp(\tilde{\alpha}_1)}{\det(\mathbf{I} + 4\tilde{\Lambda}_1)^{1/2}} \exp\left(-(\tilde{\mathbf{v}}_a - \tilde{\mathbf{v}}_b)^T (\mathbf{I} + 4\tilde{\Lambda}_1)^{-1}(\tilde{\mathbf{v}}_a - \tilde{\mathbf{v}}_b)\right)} \right]$$

$$\mathbf{H}_{ia}(\tilde{\mathbf{v}}_a) = \sum_{a=1}^M \left[1 + \frac{\det\left(\mathbf{I} - 2\tilde{\Lambda}_1^{1/2}\tilde{\Lambda}_0^{1/2}\right)^{1/2}}{\exp(\tilde{\alpha}_2)} \exp\left(-\tilde{\mathbf{u}}_i^T \tilde{\mathbf{v}}_a - \frac{1}{2}(\tilde{\Lambda}_1^{1/2}\tilde{\mathbf{u}}_i + \tilde{\Lambda}_0^{1/2}\tilde{\mathbf{v}}_a)^T B^T (\tilde{\Lambda}_1^{1/2}\tilde{\mathbf{u}}_i + \tilde{\Lambda}_0^{1/2}\tilde{\mathbf{v}}_a)\right) \right]$$

$$\left[\tilde{\Lambda}_0^{1/2} B \tilde{\Lambda}_0^{1/2} + \frac{\left(\left(0.5\tilde{\Lambda}_0^{1/2} B \tilde{\Lambda}_1^{1/2} + \mathbf{I}\right)\tilde{\mathbf{u}}_i + .5\tilde{\Lambda}_0^{1/2} B \tilde{\Lambda}_0^{1/2}\tilde{\mathbf{v}}_a\right) \left(\left(0.5\tilde{\Lambda}_0^{1/2} B \tilde{\Lambda}_1^{1/2} + \mathbf{I}\right)\tilde{\mathbf{u}}_i + 0.5\tilde{\Lambda}_0^{1/2} B \tilde{\Lambda}_0^{1/2}\tilde{\mathbf{v}}_a\right)^T}{1 + \frac{\exp(\tilde{\alpha}_2)}{\det\left(\mathbf{I} - 2\tilde{\Lambda}_1^{1/2}\tilde{\Lambda}_0^{1/2}\right)^{1/2}} \exp\left(\tilde{\mathbf{u}}_i^T \tilde{\mathbf{v}}_a + \frac{1}{2}(\tilde{\Lambda}_1^{1/2}\tilde{\mathbf{u}}_i + \tilde{\Lambda}_0^{1/2}\tilde{\mathbf{v}}_a)^T B^T (\tilde{\Lambda}_1^{1/2}\tilde{\mathbf{u}}_i + \tilde{\Lambda}_0^{1/2}\tilde{\mathbf{v}}_a)\right)} \right]^T$$

With the Taylor-expansions of the log functions, we can obtain the closed form update rule of $\tilde{\mathbf{v}}_a$ by setting the partial derivative of KL equal to 0. Then, we have

$$\tilde{\mathbf{v}}_a = \left[\left(\frac{1}{2\lambda_1} + \sum_{b=1, b \neq a}^M (y_{ba} + y_{ab}) \right) \mathbf{I} + \mathbf{H}_a(\tilde{\mathbf{v}}_a) + \frac{1}{2} \mathbf{H}_{ia}(\tilde{\mathbf{v}}_a) \right]^{-1}$$

$$\left[\sum_{b=1, b \neq a}^M (y_{ba} + y_{ab}) \tilde{\mathbf{v}}_b + \frac{1}{2} \sum_{i=1}^N y_{ia} \tilde{\mathbf{u}}_i - \mathbf{G}_a(\tilde{\mathbf{v}}_a) + \left(\mathbf{H}_a(\tilde{\mathbf{v}}_a) + \frac{1}{2} \mathbf{H}_{ia}(\tilde{\mathbf{v}}_a) \right) \tilde{\mathbf{v}}_a - \frac{1}{2} \mathbf{G}_{ia}(\tilde{\mathbf{v}}_a) \right]$$

To find the closed form updates of $\tilde{\Lambda}_0$ and $\tilde{\Lambda}_1$ we used the first-order Taylor-expansions of \mathbf{F}_i , \mathbf{F}_a and \mathbf{F}_{ia} . The gradients of \mathbf{F}_i and \mathbf{F}_{ia} with respect to $\tilde{\Lambda}_0$ are:

$$\mathbf{G}_i(\tilde{\Lambda}_0) = \sum_{i=1}^N \sum_{j=1, j \neq i}^N \left[1 + \frac{\det(\mathbf{I} + 4\tilde{\Lambda}_0)^{1/2}}{\exp(\tilde{\alpha}_0)} \exp\left(\left(\tilde{\mathbf{u}}_i - \tilde{\mathbf{u}}_j\right)^T (\mathbf{I} + 4\tilde{\Lambda}_0)^{-1} (\tilde{\mathbf{u}}_i - \tilde{\mathbf{u}}_j)\right) \right]^{-1}$$

$$4(\mathbf{I} + 4\tilde{\Lambda}_0)^{-1} \left((\tilde{\mathbf{u}}_i - \tilde{\mathbf{u}}_j)(\tilde{\mathbf{u}}_i - \tilde{\mathbf{u}}_j)^T (\mathbf{I} + 4\tilde{\Lambda}_0)^{-1} - \frac{1}{2} \mathbf{I} \right)$$

$$\mathbf{G}_{ia}(\tilde{\Lambda}_0) = \sum_{i=1}^N \sum_{a=1}^M \frac{1}{2} \left[1 + \frac{\det(B^{-1})^{1/2}}{\exp(\tilde{\alpha}_2)} \exp\left(-\tilde{\mathbf{u}}_i^T \tilde{\mathbf{v}}_a - \frac{1}{2}(\tilde{\Lambda}_1^{1/2}\tilde{\mathbf{u}}_i + \tilde{\Lambda}_0^{1/2}\tilde{\mathbf{v}}_a)^T B^T (\tilde{\Lambda}_1^{1/2}\tilde{\mathbf{u}}_i + \tilde{\Lambda}_0^{1/2}\tilde{\mathbf{v}}_a)\right) \right]^{-1}$$

$$\left[B \tilde{\Lambda}_1^{1/2} \tilde{\Lambda}_0^{-1/2} + \frac{1}{2} (\tilde{\Lambda}_1^{1/2}\tilde{\mathbf{u}}_i + \tilde{\Lambda}_0^{1/2}\tilde{\mathbf{v}}_a)^T (B + B^T) \tilde{\Lambda}_0^{-1/2} \tilde{\mathbf{z}}_a + B^T \tilde{\Lambda}_1^{1/2} \tilde{\Lambda}_0^{-1/2} B^T \right]$$

The gradients of \mathbf{F}_a and \mathbf{F}_{ia} with respect to $\tilde{\Lambda}_1$ are:

$$\mathbf{G}_a(\tilde{\Lambda}_1) = \sum_{a=1}^M \sum_{b=1, b \neq a}^M \left[1 + \frac{\det(\mathbf{I} + 4\tilde{\Lambda}_1)^{1/2}}{\exp(\tilde{\alpha}_1)} \exp\left(\left(\tilde{\mathbf{v}}_a - \tilde{\mathbf{v}}_b\right)^T (\mathbf{I} + 4\tilde{\Lambda}_1)^{-1} (\tilde{\mathbf{v}}_a - \tilde{\mathbf{v}}_b)\right) \right]^{-1}$$

$$4(\mathbf{I} + 4\tilde{\Lambda}_1)^{-1} \left((\tilde{\mathbf{v}}_a - \tilde{\mathbf{v}}_b)(\tilde{\mathbf{v}}_a - \tilde{\mathbf{v}}_b)^T (\mathbf{I} + 4\tilde{\Lambda}_1)^{-1} - \frac{1}{2} \mathbf{I} \right)$$

$$\mathbf{G}_{ia}(\tilde{\Lambda}_1) = \sum_{i=1}^N \sum_{a=1}^M \frac{1}{2} \left[1 + \frac{\det(B^{-1})^{1/2}}{\exp(\tilde{\alpha}_2)} \exp \left(-\tilde{\mathbf{u}}_i^T \tilde{\mathbf{v}}_a - \frac{1}{2} (\tilde{\Lambda}_1^{1/2} \tilde{\mathbf{u}}_i + \tilde{\Lambda}_0^{1/2} \tilde{\mathbf{v}}_a)^T B (\tilde{\Lambda}_1^{1/2} \tilde{\mathbf{u}}_i + \tilde{\Lambda}_0^{1/2} \tilde{\mathbf{v}}_a) \right) \right]^{-1} \\ \left[B \tilde{\Lambda}_0^{1/2} \tilde{\Lambda}_1^{-1/2} + \frac{1}{2} (\tilde{\Lambda}_1^{1/2} \tilde{\mathbf{u}}_i + \tilde{\Lambda}_0^{1/2} \tilde{\mathbf{v}}_a)^T (B + B^T) \tilde{\Lambda}_1^{-1/2} \tilde{z}_i + B^T \tilde{\Lambda}_0^{1/2} \tilde{\Lambda}_1^{-1/2} B^T \right]$$

With the Taylor-expansions of the log functions, we can obtain the closed form update rule of $\tilde{\Lambda}_0$ $\tilde{\Lambda}_1$ by setting the partial derivative of KL equal to 0. Then, we have

$$\tilde{\Lambda}_0 = \left[\left(\frac{1}{\lambda_0} + \frac{\sum_{i=1}^N \sum_{j=1}^N y_{ij}}{N} \right) \mathbf{I} + \frac{2}{N} \mathbf{G}_i(\tilde{\Lambda}_0) + \frac{1}{2} \mathbf{G}_{ia}(\tilde{\Lambda}_0) \right]^{-1} \\ \tilde{\Lambda}_1 = \left[\left(\frac{1}{\lambda_1} + \frac{\sum_{a=1}^M \sum_{b=1}^M y_{ab}}{N} \right) \mathbf{I} + \frac{2}{M} \mathbf{G}_a(\tilde{\Lambda}_1) + \frac{1}{2} \mathbf{G}_{ia}(\tilde{\Lambda}_1) \right]^{-1}$$

M-step: Estimate $\tilde{\alpha}_0$, $\tilde{\alpha}_1$ and $\tilde{\alpha}_2$ by minimizing the KL divergence. To find the closed form updates of $\tilde{\alpha}_0$, $\tilde{\alpha}_1$ and $\tilde{\alpha}_2$, we used second-order Taylor-expansions of the log functions and set the partial derivatives of KL with respects to $\tilde{\alpha}_0$, $\tilde{\alpha}_1$ and $\tilde{\alpha}_2$ as zeros. Then we have

$$\tilde{\alpha}_0 = \frac{\sum_{i=1}^N \sum_{j \neq i, j=1}^N y_{ij} - g_i(\tilde{\alpha}_0) + \tilde{\alpha}_0 h_i(\tilde{\alpha}_0)}{h_i(\tilde{\alpha}_0)} \\ \tilde{\alpha}_1 = \frac{\sum_{a=1}^M \sum_{b \neq a, b=1}^M y_{ab} - g_a(\tilde{\alpha}_1) + \tilde{\alpha}_1 h_a(\tilde{\alpha}_1)}{h_a(\tilde{\alpha}_1)} \\ \tilde{\alpha}_2 = \frac{\sum_{i=1}^N \sum_{a=1}^M y_{ia} - g_{ia}(\tilde{\alpha}_2) + \tilde{\alpha}_2 h_{ia}(\tilde{\alpha}_2)}{h_{ia}(\tilde{\alpha}_2)}$$

where

$$g_i(\tilde{\alpha}_0) = \sum_{i=1}^N \sum_{j=1, j \neq i}^N \left[1 + \frac{\det(\mathbf{I} + 4\tilde{\Lambda}_0)^{1/2}}{\exp(\tilde{\alpha}_0)} \exp \left((\tilde{\mathbf{u}}_i - \tilde{\mathbf{u}}_j)^T (\mathbf{I} + 4\tilde{\Lambda}_0)^{-1} (\tilde{\mathbf{u}}_i - \tilde{\mathbf{u}}_j) \right) \right]^{-1} \\ g_a(\tilde{\alpha}_1) = \sum_{a=1}^M \sum_{b=1, b \neq a}^M \left[1 + \frac{\det(\mathbf{I} + 4\tilde{\Lambda}_1)^{1/2}}{\exp(\tilde{\alpha}_1)} \exp \left((\tilde{\mathbf{v}}_a - \tilde{\mathbf{v}}_b)^T (\mathbf{I} + 4\tilde{\Lambda}_1)^{-1} (\tilde{\mathbf{v}}_a - \tilde{\mathbf{v}}_b) \right) \right]^{-1} \\ g_{ia}(\tilde{\alpha}_2) = \sum_{i=1}^N \sum_{a=1}^M \left[1 + \frac{\det(B^{-1})^{1/2}}{\exp(\tilde{\alpha}_2)} \exp \left(-\tilde{\mathbf{u}}_i^T \tilde{\mathbf{v}}_a - \frac{1}{2} (\tilde{\Lambda}_1^{1/2} \tilde{\mathbf{u}}_i + \tilde{\Lambda}_0^{1/2} \tilde{\mathbf{v}}_a)^T B (\tilde{\Lambda}_1^{1/2} \tilde{\mathbf{u}}_i + \tilde{\Lambda}_0^{1/2} \tilde{\mathbf{v}}_a) \right) \right]^{-1} \\ h_i(\tilde{\alpha}_0) = \sum_{i=1}^N \sum_{j=1, j \neq i}^N \left[1 + \frac{\det(\mathbf{I} + 4\tilde{\Lambda}_0)^{1/2}}{\exp(\tilde{\alpha}_0)} \exp \left((\tilde{\mathbf{u}}_i - \tilde{\mathbf{u}}_j)^T (\mathbf{I} + 4\tilde{\Lambda}_0)^{-1} (\tilde{\mathbf{u}}_i - \tilde{\mathbf{u}}_j) \right) \right]^{-1} \\ \left[1 + \frac{\exp(\tilde{\alpha}_0)}{\det(\mathbf{I} + 4\tilde{\Lambda}_0)^{1/2}} \exp \left(-(\tilde{\mathbf{u}}_i - \tilde{\mathbf{u}}_j)^T (\mathbf{I} + 4\tilde{\Lambda}_0)^{-1} (\tilde{\mathbf{u}}_i - \tilde{\mathbf{u}}_j) \right) \right]^{-1}$$

$$\begin{aligned}
h_a(\tilde{\alpha}_1) &= \sum_{a=1}^M \sum_{b=1, b \neq a}^M \left[1 + \frac{\det(\mathbf{I} + 4\tilde{\Lambda}_1)^{1/2}}{\exp(\tilde{\alpha}_1)} \exp\left((\tilde{\mathbf{v}}_a - \tilde{\mathbf{v}}_b)^T (\mathbf{I} + 4\tilde{\Lambda}_1)^{-1} (\tilde{\mathbf{v}}_a - \tilde{\mathbf{v}}_b) \right) \right]^{-1} \\
&\quad \left[1 + \frac{\exp(\tilde{\alpha}_1)}{\det(\mathbf{I} + 4\tilde{\Lambda}_1)^{1/2}} \exp\left(-(\tilde{\mathbf{v}}_a - \tilde{\mathbf{v}}_b)^T (\mathbf{I} + 4\tilde{\Lambda}_1)^{-1} (\tilde{\mathbf{v}}_a - \tilde{\mathbf{v}}_b) \right) \right]^{-1} \\
h_{ia}(\tilde{\alpha}_2) &= \sum_{i=1}^N \sum_{a=1}^M \left[1 + \frac{\det(B^{-1})^{1/2}}{\exp(\tilde{\alpha}_2)} \exp\left(-\tilde{\mathbf{u}}_i^T \tilde{\mathbf{v}}_a - \frac{1}{2} (\tilde{\Lambda}_1^{1/2} \tilde{\mathbf{u}}_i + \tilde{\Lambda}_0^{1/2} \tilde{\mathbf{v}}_a)^T B (\tilde{\Lambda}_1^{1/2} \tilde{\mathbf{u}}_i + \tilde{\Lambda}_0^{1/2} \tilde{\mathbf{v}}_a) \right) \right]^{-1} \\
&\quad \left[1 + \frac{\exp(\tilde{\alpha}_2)}{\det(B^{-1})^{1/2}} \exp\left(\tilde{\mathbf{u}}_i^T \tilde{\mathbf{v}}_a + \frac{1}{2} (\tilde{\Lambda}_1^{1/2} \tilde{\mathbf{u}}_i + \tilde{\Lambda}_0^{1/2} \tilde{\mathbf{v}}_a)^T B (\tilde{\Lambda}_1^{1/2} \tilde{\mathbf{u}}_i + \tilde{\Lambda}_0^{1/2} \tilde{\mathbf{v}}_a) \right) \right]^{-1}
\end{aligned}$$

The VBEM approach for LSMH-I is similar to the VBEM approach for LSMH with the exception of $\tilde{\alpha}_a$, $a = 1, 2, \dots, M$ replacing $\tilde{\alpha}_2$. Therefore, the closed form update rule for $\tilde{\alpha}_a$ is

$$\tilde{\alpha}_a^{(t+1)} = \frac{\sum_{i=1}^N y_{ia} - g_{ia}(\tilde{\alpha}_a^{(t)}) + \tilde{\alpha}_a^{(t)} h_{ia}(\tilde{\alpha}_a^{(t)})}{h_{ia}(\tilde{\alpha}_a^{(t)})}$$

where

$$\begin{aligned}
g_{ia}(\tilde{\alpha}_a) &= \sum_{i=1}^N \left[1 + \frac{\det(B^{-1})^{1/2}}{\exp(\tilde{\alpha}_a)} \exp\left(-\tilde{\mathbf{u}}_i^T \tilde{\mathbf{v}}_a - \frac{1}{2} (\tilde{\Lambda}_1^{1/2} \tilde{\mathbf{u}}_i + \tilde{\Lambda}_0^{1/2} \tilde{\mathbf{v}}_a)^T B (\tilde{\Lambda}_1^{1/2} \tilde{\mathbf{u}}_i + \tilde{\Lambda}_0^{1/2} \tilde{\mathbf{v}}_a) \right) \right]^{-1} \\
h_{ia}(\tilde{\alpha}_a) &= \sum_{i=1}^N \left[1 + \frac{\det(B^{-1})^{1/2}}{\exp(\tilde{\alpha}_a)} \exp\left(-\tilde{\mathbf{u}}_i^T \tilde{\mathbf{v}}_a - \frac{1}{2} (\tilde{\Lambda}_1^{1/2} \tilde{\mathbf{u}}_i + \tilde{\Lambda}_0^{1/2} \tilde{\mathbf{v}}_a)^T B (\tilde{\Lambda}_1^{1/2} \tilde{\mathbf{u}}_i + \tilde{\Lambda}_0^{1/2} \tilde{\mathbf{v}}_a) \right) \right]^{-1} \\
&\quad \left[1 + \frac{\exp(\tilde{\alpha}_a)}{\det(B^{-1})^{1/2}} \exp\left(\tilde{\mathbf{u}}_i^T \tilde{\mathbf{v}}_a + \frac{1}{2} (\tilde{\Lambda}_1^{1/2} \tilde{\mathbf{u}}_i + \tilde{\Lambda}_0^{1/2} \tilde{\mathbf{v}}_a)^T B (\tilde{\Lambda}_1^{1/2} \tilde{\mathbf{u}}_i + \tilde{\Lambda}_0^{1/2} \tilde{\mathbf{v}}_a) \right) \right]^{-1}
\end{aligned}$$

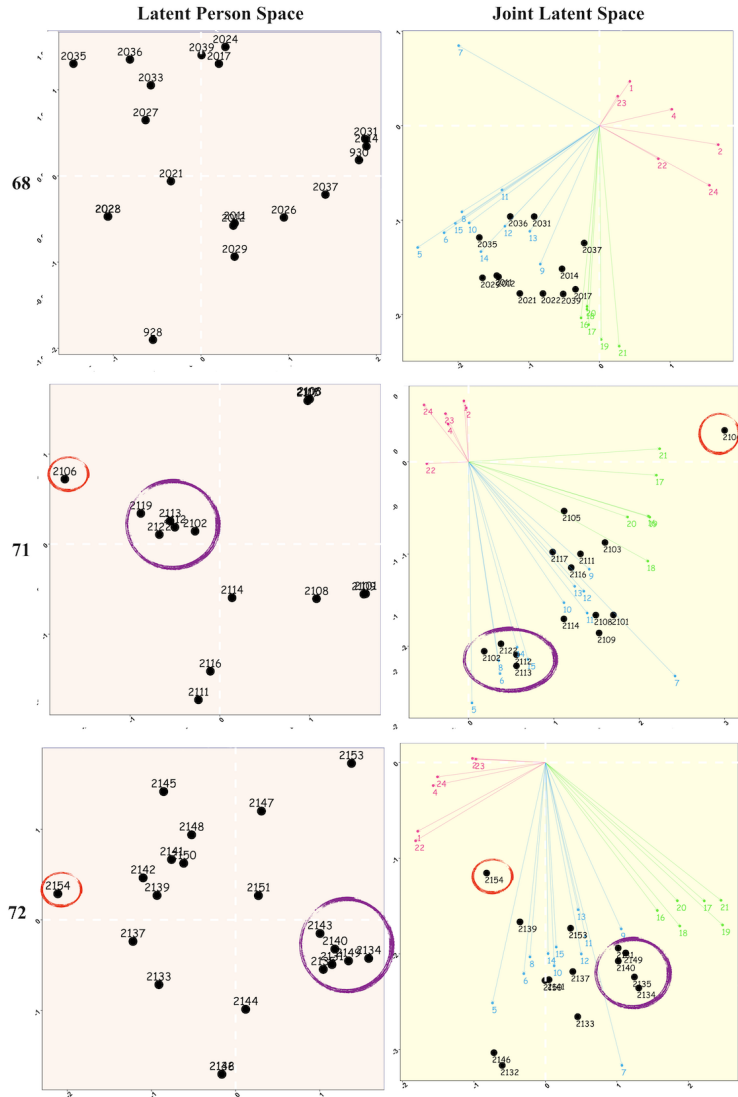


Figure 17: The Latent Spaces

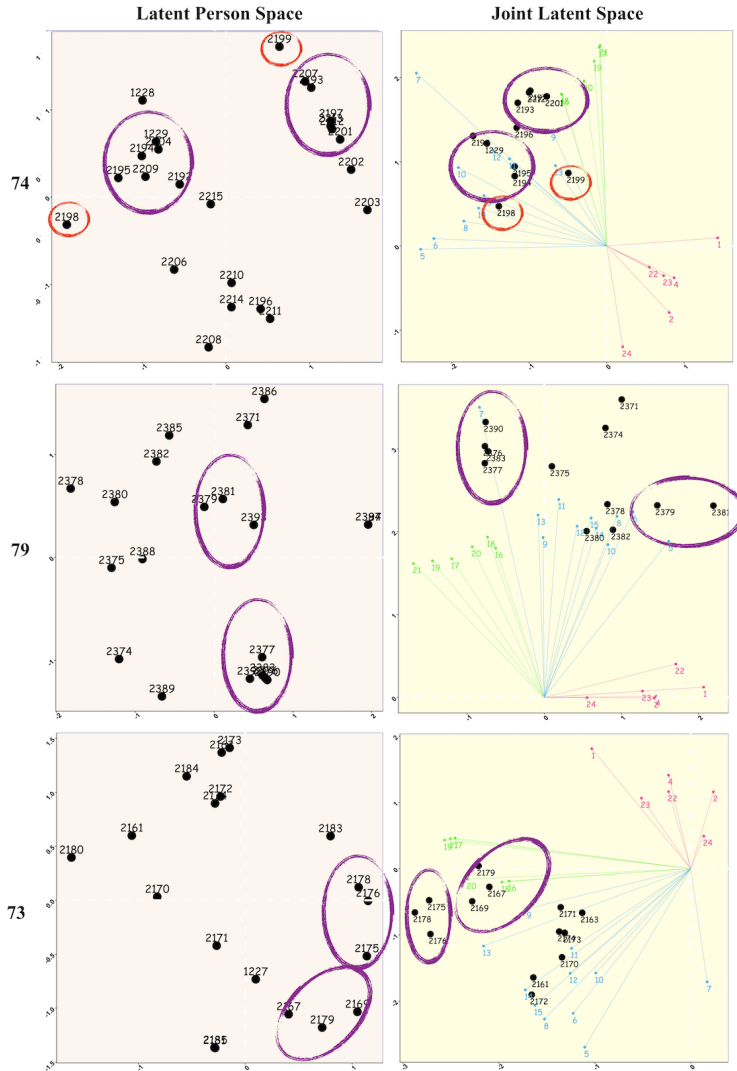


Figure 18: The Latent Spaces